Sheffield Hallam University

Experimental study and modelling of average void fraction of gas-liquid two-phase flow in a helically coiled rectangular channel

XIA, Guodong, CAI, Bo, CHENG, Lixin, WANG, Zhipeng and JIA, Yuting

Available from Sheffield Hallam University Research Archive (SHURA) at:

https://shura.shu.ac.uk/18593/

This document is the Accepted Version [AM]

Citation:

XIA, Guodong, CAI, Bo, CHENG, Lixin, WANG, Zhipeng and JIA, Yuting (2018). Experimental study and modelling of average void fraction of gas-liquid two-phase flow in a helically coiled rectangular channel. Experimental Thermal and Fluid Science, 94, 9-22. [Article]

Copyright and re-use policy

See http://shura.shu.ac.uk/information.html

Sheffield Hallam University Research Archive
http://shura.shu.ac.uk

Experimental study and modelling of average void fraction of gas-liquid two-phase flow in a helically coiled rectangular channel

Guodong Xia[a*] Bo Cai[a] Lixin Cheng[a,b*] Zhipeng Wang[a] Yuting Jia[a]

[a]College of Environmental and Energy Engineering, Beijing University of Technology, Beijing, 100124, China

[b]Department of Engineering and Mathematics, Faculty of Arts, Computing, Engineering and Sciences, Sheffield Hallam University, UK

*Corresponding author: Tel.:+86 10 67391985-8301; fax: +86 10 67391983. *Email address: xgd@bjut.edu.cn; lixincheng@hotmail.com

Abstract

Void fraction is an important parameter in designing and simulating the relevant gas-liquid two-phase flow equipment and systems. Although numerous experimental research and modelling of void fraction in straight circular channels have been conducted over the past decades, the experimental data and prediction methods for the average void fraction in helically coiled channels are limited and needed. Especially, there is no such information in helically coiled channels with rectangular cross section. Therefore, it is essential to advance the relevant knowledge through experiments and to develop the corresponding prediction methods in helically coiled rectangular channels. This paper presents experimental results of the average void fraction and new models for the void

fraction in a horizontal helically coiled rectangular channel. First, experiments were conducted with air-water two-phase flow in the horizontal helically coiled rectangular channel at a wide range of test conditions: the liquid superficial velocity ranges from 0.11 to 2 m/s and the gas superficial velocity ranges from 0.18 to 16 m/s**.** The average void fractions were measured with a quick-closing valve (QCV) method. The measured void fraction ranges from 0.012 to 0.927 which cover four flow regimes including unsteady pulsating, bubbly, intermittent and annular flow observed with a high speed camera. Second, comparisons of the entire measured average void fraction data to 32 void fraction models and correlations were made. It shows a low accuracy of these models and correlations in predicting the experimental data for the void fraction smaller than 0.5 while the drift flux model of Dix [Woldesemayat and Ghajar, Int. J. Multiphase Flow. 33 (2007) 347-370.] predicts 98.3% of the entire experimental data within ±10% for the void fraction larger than 0.5. Therefore, the Dix model is recommended for the void fraction larger than 0.5. Furthermore, the observed flow regimes in the coiled channels were compared to two mechanistic flow regime maps developed for horizontal straight circular tubes. The flow regime maps do not capture all flow regimes in the present study. Finally, the effects of the limiting affecting parameters on the void fraction models are analyzed according to the physical phenomena and mechanisms. Incorporating the main affecting parameters, new void fraction models have been proposed for the void fractions in the ranges of $0 < \alpha \leq 0.2$ and $0.2 < \alpha \leq 0.5$ respectively according to the slip flow model. Both models predict the experimental data reasonably well. Overall, the new proposed models and the recommended model predict 92.8% of the entire void fraction data within ±30%.

Keywords: air-water two-phase flow; helically coiled rectangular channel; flow regime; void fraction; experiment; model

1. Introduction

Gas-liquid two-phase flow in helically coiled channels is frequently encountered in various industrial units such as various heat exchangers, power generations, nuclear reactors, oil-gas process systems, gas-liquid mixing units and so on [1, 2]. Understanding the channel average void fraction of two-phase flow is significant and necessary for modelling the flow regimes and their transitions, the two-phase pressure drop and phase change heat transfer in various gas-liquid two-phase flow systems [3-5]. Accurate knowledge of the average void fractions of gas-liquid two-phase flow is significant in modelling the numerical computation and beneficial to the design and application for various industrial processes.

A number of researchers have conducted experimental investigations on the void fraction in straight circular tubes under various conditions such as flow boiling, condensation and adiabatic two-phase flow. Srisomba and Mahian [6] conducted the experiments to measure the void fraction of R-134a in a horizontal circular tube using a quick-closing valve (QCV) method and optical observation techniques. Based on their measured void fraction, they have proposed new correlations for predicting the void fraction for different flow regimes. Oliviera [7] investigated the effects of the inclination

angles on the void fraction, which closely related with flow regimes during condensation with R134a inside smooth tubes. Jagan and Satheesh [8] investigated the flow regimes and the void fraction of air-water two-phase flow in a circular tube at different inclination angles ranging from 0° to 90°. The void fractions were measured using the QCV method in their study. Milkie [9] investigated the flow regimes and void fractions for condensation of propane flowing through horizontal tubes with a diameter of 7 mm and 15 mm. Detailed analyses of the video frames were used to develop a new multi-regime void fraction model based on the drift flux model. The model provides improved agreement with the experimental results when compared to correlations in the literature. Lockanathan and Hibiki [10] presented a comprehensive review and analysis of the flow regime, void fraction and pressured drop for downward two-phase flow and pointed out the future research needs in their review. Just to name a few studies of void fraction in straight tubes here. Furthermore, the available prediction models and correlations for the void fraction in the two-phase flow have been extensively developed for straight circular channels [11].

However, studies of the void fraction of gas-liquid two-phase flow in helically coiled channels are very limited. Due to the centrifugal acceleration effect which generating the secondary flow in the main two-phase flow, the flow structure and the relative motion between phases in a helically coiled channel are much more complicated than those in a straight tube. In particular, studies of the void fraction and flow structure for gas-liquid two-phase flow in a helically coiled rectangular channel are very limited in the literature so far. Recently, Liu et al. [15] investigated the characteristics of air-water two-phase flow in a vertical helically coiled rectangular channel and observed the phase distribution and fluid

structure using a high speed video system. They indicated that the presence of the secondary flow leading to a complex asymmetry phase distribution for two-phase flow in the helically coiled rectangular channels. They illustrated the flow pattern evolutions in different position of the helically coiled rectangular channels. However, their study does not concern the void fraction in the helically coiled rectangular channels, which is important in understanding the fundamentals of gas-liquid two-phase flow and worth being investigated in such a coiled channel with non-circular shape.

Furthermore, there are many void fraction correlations/models available in the literature. Based on the major three typical models, i.e. homogeneous model, slip flow model and drift flux model. Many models and correlations for predicting the void fraction were developed based on these models. Woldesemayat and Ghajar [11] investigated the predictive performance of 68 void fraction models and correlations for straight tube with different orientations. Xue [12] did a comparative work to evaluate the accuracy of 39 models and correlations for calculating void fraction in downward two-phase flow system. Jagan and Satheesh [8] measured void fraction in straight tubes under different inclined angles and compared with five existing correlations. Mandal and Das [13] and Biswas and Das [14] investigated the two-phase pressure drop and the liquid holdup with three varying gas-non-Newtonian two-phase flow for both horizontal and vertical helical coils with circular cross section. They presented the void fraction correlations for helically coiled channel by dimensionless analysis. Furthermore, Xia and Liu [15-17, 36] investigated the effect of liquid holdup on the phase distribution and pressure drop of two-phase flow in helically coiled rectangular channel only by the numerical simulation method. However,

nearly all the available void fraction models and correlations of air-water two-phase flow were developed for straight circular tubes. It is unclear if these correlations are applicable to helically coiled rectangular channels. Furthermore, flow regimes are intrinsically related to the corresponding void fractions. It is essential to predict the flow regimes properly using the relevant flow regime map when developing the relevant prediction methods for the void fractions. Several mechanistic flow regime models and maps have been developed for flow regime pattern prediction, i.e. the mechanistic maps and models of Taitel and Dukler [53], Taitel [54] and Zhang et al. [55-57]. These maps and models are generally applicable to straight circular channels. For the flow regimes in the coiled rectangular channels in the present study, it is essential to evaluate the mechanistic flow regime maps and models with the experimental data in such channels. Due to the secondary flow generated in the coiled channels, possible different flow regimes may occur in such channels.

To the authors' knowledge based on the literature review, the experimental data and prediction methods for the average void fraction of two-phase flow in helically coiled channels are limited. Especially, there is no such information in helically coiled channels with rectangular cross section so far. Therefore, it is essential to conduct experiments to measure the average void fractions of gas-liquid two-phase flow in the helically coiled rectangular channels and to develop new models for predicting the void fraction if the existing models do not work, which are the objectives of the present study.

In this study, the experimental results of the average void fractions corresponding to the flow regimes observed with the high speed video camera are presented at first. Then, 32 selected models and correlations for the void fraction have been evaluated with the

measured void fraction data. Furthermore, the mechanistic flow regime maps of Taitel and Dukler [53] and Zhang et al. [55, 56] have been evaluated with the observed flow regimes in the coiled channel. Finally, new models have been proposed for the helically coiled rectangular channel according to the void fraction ranges and the relevant physical phenomena and mechanisms.

2. Experimental setup, test section and measurement system

An experimental system was designed and built to measure the average void fractions and to observe the flow regimes of air-water two-phase flow in the horizontal helically coiled rectangular channel simultaneously by the QCV method and the flow visualization method with the high speed video camera respectively. The experimental setup, test section and measurement system are described here.

2.1. Experimental setup

Figure 1 shows the schematic diagram of the experimental setup for air-water two-phase flow for the measurement of the void fraction in the test channel. It consists of air and water supply system including pipes and valves (8), (9) and (10), the test section (7), measurement system and data acquisition system including a data acquisition unit (12) and a computer (13). The types, modes and manufactures of the instrument and equipment used in the experiments are shown in Table 2. Water is supplied by a centrifugal pump (2) from a water tank (1) having a volume of 1 m^3. Air is supplied by the air screw compressor (4) and

then stored in the air reservoir (5) at a pressure of 0.8 Mpa. The reservoir (5) is used to maintain stable air flow in the experimental system. The flow rate of air is measured by three gas flow-meters (6) with an accuracy of ±1.5%. The flow rate of water is measured by an electromagnetic flow-meter (3) with an accuracy of ±0.5%. The water flow rate can be adjusted with an adjustable valve in the water supply line to a desired superficial liquid velocity in the experiments. The three flow meters are used to achieve the wide range test range of superficial velocities from low to high values. Three values after the gas flow meters are used to adjust the air flow rate to a desired gas superficial velocity in the experiments. Air and water are well mixed in a Y-connection mixer before the test section, which has a straight branch for liquid flow and air injected in the side-way. Then, the air-water two-phase mixtures flow into the test section (7) which is the horizontal helically coiled rectangular channel, where the QCV method including two solenoid valves (8) and (9) is used to measure the average void fraction and the Motion Pro X4 high speed video camera (11) is used to observe the flow regimes simultaneously. The pipe between the Y-mixer and the test section is long enough to ensure that the gas-liquid two-phase flow is stable in the experiments. Finally, the two-phase fluids flow back to the water tank which is open to the atmosphere. The water returns to the water tank (1) and the air vents into the atmosphere.

2.2. Test section

The test section is a transparent helically coiled rectangular channel which is made of plexiglass as shown in Figure 2. Figure 3 shows the schematic diagram of the helically

coiled rectangular channel and its geometry dimensions. Table 1 lists the geometry dimensions of the test section corresponding to Figure 3. The coil diameter D of the helically coiled rectangular channel is 141 mm and its pitch P is 140 mm. The helix angle of the test section is 17.5º. The dimensions of its rectangular cross-section is: $w \times h$ = 25 mm (width) × 34 mm (height). For the non-circular channel, equivalent diameters rather than hydraulic diameters is used in gas-liquid two-phase flow as suggested by Cheng et al. [18-20] and Moreno Quibén et al. [21, 22]. The equivalent diameter d_E of the rectangular channel is defined as

$$d_E = \sqrt{\frac{4A_R}{\pi}} = \sqrt{\frac{4wh}{\pi}} \tag{1}$$

where A_R is the cross-section area of the rectangular coiled channel. It should be pointed out that using the equivalent diameter gives the same mass velocity as in the non-circular channel and thus correctly reflects the mean liquid and vapor velocities, something using hydraulic diameter in a two-phase flow does not [18-22].

2.3. Measurement system

The measurement system consists of flow meters for the liquid and gas flow rates, measurements of the average void fractions with the QCV method and observing the corresponding flow regimes with the high speed video camera simultaneously. The sampling frequency of the high speed video camera is 1000 frames per second. The resolution of acquired frames is 512 × 512 pixel. The measured parameters were acquired

by the Agilent 34972A data acquisition system (DAS) and a computer. The measured data were stored in the computer for future data reduction and analysis.

Figure 4 shows the principle of measuring the void fraction with the QCV method. Two normally opened solenoid valves (8) and (9) are mounted at the inlet and the outlet of the test section respectively. One normally closed solenoid valve (10) is mounted in the bypass line. The three solenoid valves can function simultaneously while the same power supply is connected to the three actuators of the solenoid valves.

The channel average void fraction of gas-liquid two-phase flow in the tested helically coiled rectangular channel with the QCV method can be calculated as follows:

$$\alpha = \frac{1}{n}\sum_{i=1}^{n}\left(1-\frac{M_i}{M}\right) \tag{2}$$

where M is the mass of water filled in the test section, M_i is the water mass of two-phase flow remained in the test section, n is the number of measurements at a given flow condition. The mass of water remaining in the channel is measured by using an electronic balance with high accuracy. The measurements are repeated at least five times for each test run and the average result of all the measurements for the test run is used as the measured average void fraction.

2.4. Experimental conditions and measurement uncertainty analysis

Experiments were conducted with air-water two-phase flow at a temperature of 20℃.

The density of water and air are 998.2 and 1.205 kg/m^3 respectively and the dynamic viscosity of water and air are 1.004×10^{-3} and 1.81×10^{-5} m^2/s respectively. Wide ranges of liquid and gas superficial velocities were used to cover a wide range void fractions in various flow regimes in the test section. Table 3 lists the experimental conditions. The liquid superficial velocity varies from 0.11 to 2 m/s and the gas superficial velocity varies from 0.18 to 16 m/s. With the test conditions, the channel average void fraction is in the range from 0.012 to 0.927.

The measurement uncertainties were analyzed with the methods of Taylor [23] in this study. Table 3 shows the uncertainties of measurement parameters. The processing precision of channel width and height is less than 0.5 mm. the uncertainty of channel cross-section area is estimated to be about ±1.18%. The uncertainty of the liquid superficial velocity is ± 3.22%. The uncertainty of the gas superficial velocity is ± 5.99%. The uncertainty of channel average void fraction is ± 2.8%.

3. Experimental results and analysis

The average void fraction of gas-liquid two-phase flow were measured in the horizontal helically coiled rectangular channel by using the QCV method in wide range of gas and liquid superficial velocities: $0.18 < U_{SG} < 16$ m/s and $0.1 < U_{SL} < 2$ m/s. The corresponding flow regimes were simultaneously observed with the high speed video camera. Four main flow regimes were observed in the test helically coiled rectangular channel, i.e. the unsteady pulsating flow, the bubbly flow, the intermittent flow and the

annular flow.

Figure 5 shows the measured average void fractions at the liquid superficial velocities of 0.098, 0.196 and 0.294 m/s and a photograph of the observed unsteady pulsating flow regime which occurs at a medium range of the void fraction from about 0.3 to 0.75. Figure 6 shows the measured average void fractions at the liquid superficial velocities of 0.882, 0.98, 1.378 and 1.905 m/s and a photograph of the observed the bubbly flow regime which occurs at a low range of the void fraction from about 0.008 to 0.18. Figure 7 shows the measured average void fractions at the liquid superficial velocities of 0.196, 0.392, 0.588 and 0.784 m/s and a photograph of the observed intermittent flow regime which occurs at a wide range of void fraction from about 0.18 to 0.83. Figure 8 shows the measured average void fractions at the liquid superficial velocities of 0.098, 0.196, 0.392, 0.588 m/s and a photograph of the observed annular flow regime which occurs at a higher void fraction larger than 0.73. There is a correlation between the flow regimes and the average void fraction according to the experimental results.

Figure 9 shows the comparison of the measured average void fraction at various conditions for the four flow regimes as shown in Figs. 5 to 8. Apparently, the observed flow regimes are also significantly affected by the liquid and gas superficial velocities. With increasing the liquid superficial velocity, the channel average void fraction decreases at a constant gas superficial velocity. At a lower gas superficial velocity of $U_{SG} < 4$ m/s, the channel average void fraction increases fast with increasing the gas superficial velocity for all the flow regimes. With further increasing the gas superficial velocity, the channel average void fraction increases slowly for the flow regimes of intermittent flow and annular

flow regime (Other flow regimes are not observed at higher gas superficial velocities). When the gas superficial velocity U_{SG} is smaller than 8 m/s, the flow regimes observed in the horizontal helically coiled rectangular channel are the unsteady pulsating flow, the bubbly flow and the intermittent flow. The channel average void fractions in these three flow regimes are significantly affected by the gas and liquid superficial velocities. When the gas superficial velocity U_{SG} is higher than 8 m/s, the observed flow regime is the annular flow. The liquid superficial velocity U_{SL} has a significant effect on the channel average void fraction in the annular flow regime.

From the experimental results, it is obtained that the average void fraction are not only correlated with the flow regimes but also related to the gas and liquid superficial velocities.

4. Comparison of the measured average void fractions to 32 selected void fraction models and correlations

Since the research on the void fraction in helically coiled rectangular channels is very limited, it is unclear if the available void fraction models and correlations work for the measured void fraction in such channels. Furthermore, nearly all the available void fraction models and correlations were developed for straight circular tubes. Therefore, it is essential to examine the available void fraction models and correlations with the experimental void fraction data in the coiled rectangular channel. 32 void fraction models and correlations are used to compare to the measured void fractions in the horizontally helically coiled rectangular channels in this study. Taking into account the effect of the average void

fraction on the two-phase mixture density, this influence is of different magnitude for different ranges of the void fraction according to the study by Ghajar and Bhagwat [24]. Adopting the approach of Ghajar and Bhagwat [24], the performance of the selected models and correlations are assessed within certain error bands criterion of ±30%, ±20%, and ±10% for three different ranges of the average void fraction namely, $0 < \alpha \leq 0.2$, $0.2 < \alpha \leq 0.5$, $0.5 < \alpha \leq 1$, respectively. According to the study of Woldesemayat and Ghajar [11], the selected void fraction models and correlations considered in our study are classified into four categories, i.e. the homogeneous models, the slip flow models, the drift flux models and other empirical correlations which are listed in Tables 4 to 7, respectively.

4.1. The homogeneous models for the void fraction

The general form of the homogeneous model may be generally expressed as a constant or a multiple function of the homogeneous void fraction α_{H} as follows:

$$\alpha = K\alpha_{\mathrm{H}} \tag{5}$$

Various homogenous models were developed for predicting the void fraction in gas-liquid two-phase flow. Table 4 lists 5 selected homogeneous models for the void fraction, which are used to compare to the experimental data obtained in the experiments. Figure 10 shows the comparative results of the entire experimental data to the five homogenous models in Table 4. According to the statistical results, the best three homogeneous models for the three void fraction ranges are given in Table 8. For the void fractions in the first range of 0

$< \alpha \leq 0.2$, all five models show a poor predictive capability to capture the experimental void fractions. The best method is the model of Czop et al. [28]. However, it only predicts 17.6% of the total experimental data points within ±30% while other models predict no data within ±30%. For the void fractions in the second range of $0.2 < \alpha \leq 0.5$, the top performing model comes from Nishino and Yamazaki [25] being able to predict 55% of the experimental data within ±20%, followed by the models of Czop et al. [28] and Chisholm [27] being able to predict 30% and 25% of the experimental data within ±20%. None of the models are good enough to predict the void fraction. For the void fractions in the last range of $0.5 < \alpha \leq 1$, the best prediction method is also the model proposed by Nishino and Yamazaki [25], which is capable of predicting 93.2% of the total experimental data points within ±10%. The models of Czop et al. [28] and Chisholm [27] predict 83.1% and 76.3% of the total data points within ±10% respectively.

From the comparative results, it can be found that for the void fraction less than 0.5, none of the selected homogenous models work for the experimental data in the horizontal helically coiled rectangular channel. For the void fraction larger than 0.5, the model of Nishino and Yamazaki [25] is able to predict the experimental data reasonably well. Therefore, new model is needed for the void fraction less than 0.5.

4.2. The slip flow models for the void fraction

For the homogeneous flow model, equal velocities of two phases is assumed, it means that the slip ratio S of two phases is equal to unity. However, in the real two-phase flow, there is a slip between the gas and liquid phases, i.e., $S \geq 1$ or $S < 1$, which depends upon

the fluid properties, flow regimes, pipe shapes and structures and pipe orientations. Therefore, it is essential to consider the slip ratio in modelling the complex gas-liquid two-phase flow.

From the available model in the literature, various forms of the slip models are available. One general form of the slip flow model for the void fraction may be expressed as follows:

$$\alpha = \frac{1}{1+\left(\frac{1-x}{x}\right)\left(\frac{\rho_g}{\rho_l}\right)S} \tag{6}$$

where the ratio of the liquid and gas mass fractions and the ratio of gas and liquid densities are correlated in the model.

Incorporating the effect of the liquid and gas dynamic viscosities in the model, the general form of the slip flow model accounting for the slip may be expressed as follows:

$$\alpha = \frac{1}{1+A\left(\frac{1-x}{x}\right)^p\left(\frac{\rho_g}{\rho_l}\right)^q\left(\frac{\mu_l}{\mu_g}\right)^r} \tag{7}$$

Various forms of the slip flow models for the void fraction have been developed so far. Table 5 lists 11 slip flow models for the void fraction, which are used to compare to the experimental void fraction data obtained in the experiments.

Figure 11 shows the comparative results of the entire experimental data to the selected

11 slip models for the void fraction in Table 5. According to the statistical results, the best three slip flow models for the three void fraction ranges are given in Table 8. For the void fraction in the first range of $0 < \alpha \leq 0.2$, the models of Zivi [32] and Turner and Wallis [33] predict 41.2% of the entire void fraction data points within ±30%. The model of Thom [31] predicts only 23.5% of the entire void fraction data points within ±30%. None of these models predict the experimental data satisfactorily in this void fraction range. For the void fraction in the second range of $0.2 < \alpha \leq 0.5$, The model of Hamersma and Hait [39] predicts 75% of the entire experimental void fraction data points within ±20% while the models of Lockhart and Martinelli [29] and Spedding and Chen [37] predict 65% and 60% of the entire experimental data points within ±20%. Again, all the three models are not good enough for predicting the experimental void fractions. For the void fraction in the last range of $0.5 < \alpha \leq 1$, the best agreement between the experimental and the predicted data is given by the model Spedding and Chen [37], followed by those of Chen [38] and Smith [35], which predict 93%, 88.1% and 81.4% of entire experimental data points within ±20% respectively.

As the void fraction is less than 0.5 none of the selected slip flow models work better for the experimental data in the horizontal helically coiled rectangular channel than the homogeneous model. However, the predictions are not good enough and the models need to be improved. For the void fraction larger than 0.5, all the three models predict the experimental data reasonably well. The model of Spedding and Chen [37] gives the best predictive results and may be recommended for the void fraction calculation in this range.

4.3. The drift flux models for the void fraction

The drift flux model assumes one phase dispersed in the other continuous phase and requires determination of the distribution parameter and drift velocity as variables to calculate the void fraction. The drift flux model for the void fraction is expressed as follows:

$$\alpha = \frac{U_{SG}}{C_o U_M + U_{gm}} \tag{8}$$

where

$$U_M = U_{SG} + U_{SL} \tag{8a}$$

In this model, the distribution C_0 and the drift velocity U_{gm} need to be determined in order to predict the void fraction. Various methods for calculating the two parameters have been proposed by various researchers so far. Table 6 lists 12 drift flux models for the void fraction, which are used to compare to the experimental data obtained in the experiments.

Figure 12 shows the comparative results of the entire experimental void fraction data to the selected 12 drift flux models listed in Table 6. According to the statistical results, the best three drift flux flow models for the three void fraction ranges are given in Table 8. For the void fraction in the first range of $0 < \alpha \leq 0.2$, all 12 models show a poor predictive capability to capture the experimental void fraction data. The best method is the model of Bestion [46]. However, it only predicts 23.5% of the total experimental data points within ±30%. No model can predict the void fraction satisfactorily in this range. For the void

fractions in the range of $0.2 < \alpha \leq 0.5$, the best method is the model of Mishima and Hibiki [48] which predicts 60% of the entire experimental void fraction data points within ±20%. The models of Mattar and Gregory [47] and Jowitt et al. [45] predict 55% and 35% of the entire experimental data within ±20%, respectively. Apparently, no model can predict the void fraction satisfactorily in this void fraction range. For the void fractions in the range of $0.5 < \alpha \leq 1$, the best method is the model of Dix (Woldesemayat and Ghajar [11]) which predicts 98.3% of the total experimental void fraction data points within ±10%. The models of Jowitt et al. [45] and Rouhani and Axelsson [41] predict 79.7% of the entire data points within ±10%.

For the void fraction less than 0.5, none of the selected drift flux models work well for the void fractions in the helically coiled rectangular channel. For the void fraction larger than 0.5, the model of Dix (Woldesemayat and Ghajar [11]) gives the best predictive results. Therefore, it is recommended for the void fraction in this range.

4.4. Other empirical correlations for the void fraction

Other miscellaneous empirical correlations for the void fraction have been developed by various researchers. Table 7 lists 4 empirical correlations for the void fraction, which are used to compare to the experimental data obtained in the experiments.

Figure13 shows the comparative results of the entire experimental void fraction data to the selected 4 empirical correlations in Table 7. According to the statistical results, the best three empirical correlations for the three void fraction ranges are given in Table 8. For the void fraction in the first range of $0 < \alpha \leq 0.2$, all four empirical correlations show a poor

predictive capability to capture the experimental void fraction data. Of the four correlations, the best method is the correlation of the Hart et al. [49]. However, it only predicts 29.4% of the entire experimental void fraction data points within ±30%. The Neal and Bankoff [51] correlation only predicts 11.8% of the entire experimental data points within ±30%. For the void fraction in the second range of $0.2 < \alpha \leq 0.5$, all four empirical correlations show a poor predictive capability to capture the experimental void fraction data. The best method is the correlation of Huq and Loth [50] which only predicts 40% of the total experimental data points within ±20%. Other three correlations poorly predict the experimental data. The correlation of Neal and Bankoff [51] predicts 15% of the total experimental data points while the correlation of Hart [49] only predicts 5% of the total experimental data within ±20%. The correlation of Cioncoloni and Thome [52] predicts no data in this void fraction range. For the void fractions in the last range of $0.5 < \alpha \leq 1$, the best prediction method is the model proposed of Huq and Loth [50], which predicts 88.1% of the total experimental data points within ±10%. The Cioncoloni and Thome [52] correlation predicts 78% of the entire experimental data points within ±10% while the Hart et al. [49] correlation only predicts 35.6% of the entire e data within ±10%.

For the void fraction less than 0.5, none of the selected empirical correlations work for the experimental data in the horizontal helically coiled rectangular channel. For the void fraction larger than 0.5, the correlations of Huq and Loth [50] and Cioncoloni and Thome [52] predict the experimental data reasonably well.

According to the afore-going comparative results, it is clear that none of the models and correlations satisfactorily predicts the void fraction data in the range of $0 < \alpha \leq 0.2$. For

the void fraction in the range of $0.2 < \alpha \leq 0.5$, no models and correlations capture the experimental data well. The model of the Hamersma and Hait [39] predicts 75% of the entire data, but it is not good enough. Therefore, it is essential to propose new models for the void fraction in these two ranges. For the void fraction in the range of $0.5 < \alpha \leq 1$, several models are able to predict the experimental data. The top three methods are the models of Dix (Woldesemayat and Ghajar [11]), Spedding and Chen [37] and Nishino and Yamazaki [25]. Therefore, these methods may be recommended for the prediction of the void fraction in the horizontal helically coiled rectangular channel.

5. Evaluation of the mechanistical flow regime maps and models with the observed flow regimes in the coiled rectangualr channel

Several mechanistic flow regime maps and models have been developed for predicting flow regimes in straight circular channels [53-57]. It is essential to evaluate these maps and models with new experimental flow regime data. Two mechanistic flow regime maps and models of Taitel and Dukler [53] and Zhang et al. [55-56] for horizontal two-phase flow are selected to compare with the experimental flow regime data in the coiled rectangular channel in the present study. Figures 14 and 15 show the experimental flow regime data compared with flow regime maps reported by Taitel and Dukler [53] and Zhang et al. [55-56] respectively. There are five flow regimes including dispersed bubbly, slug, stratified, wave and annular flow for horizontal air-water flow. It can be seen that the bubbly-to-slug flow transition occurs at a lower superficial liquid velocity and the

slug-to-annular transition occurs at a lower superficial gas velocity for the experimental flow regime data in the coiled channel. Both flow regime maps do not capture the bubbly flow and annular flow regimes while they predict the intermittent flow regimes reasonably well. Furthermore, a new type of flow regime named unsteady pulsating flow was observed in the coiled channel in the present study. It can be seen that both unsteady pulsating flow and stratified flow are in the left bottom corner of both flow regime maps. However, unsteady pulsating-to-slug transition occurs at high liquid superficial flow velocities in horizontal helically coiled channel. Due to the new flow regime observed in the coiled channel, it seems that it is difficult to apply the existing flow regime maps to this new flow regime which is not defined in the flow pattern maps.

Although the selected mechanism flow regime maps and models have considered the effects of operational parameters, geometrical parameters and the physical properties of the fluids, these mechanistic maps and models do not work for the experimental flow regime transitions in the coiled channels due to the non-circular channel and secondary flow generated in the coiled channel. As a result, the corresponding void fraction models developed for straight circular tubes are not applicable to the horizontal helically coiled channel. However, it should be pointed out that effort should be made to develop mechanistic maps and models for coiled channels in future. In order to achieve it, extensive experimental data are needed and thus experimental work should be further conducted for various channel size, arrangement and a wide range of experimental conditions.

6. New models for the void fraction in the horizontal helically coiled channel

In order to understand the physical phenomena and mechanisms of the void fraction and propose new models based on the phenomena mechanisms for the coiled channel, the existing void fraction models have been analyzed here and the limiting affecting parameters have been identified at first. Then, new models have been proposed considering the phenomena, mechanisms and the limiting parameters in the coiled channels.

6.1. Analysis of the existing models for the void fraction

Woldesemayat and Ghajsr [11] and Ghajar and Bhagwat [24] tried to develop generalized void fraction models and correlations which could acceptably handle all void fraction data in straight tubes regardless of the flow patterns and inclination angles for gas-liquid two-phase flow. However, evaluation of such generalized void fraction models and correlations indicates a lack of ability of these models and correlations to satisfactorily predict the void fraction data independence of the flow regimes and mixture flow rates.

For the void fraction in the horizontal helically coiled rectangular channel, it is worth noting that the 32 selected models and correlations fail to adequately predict data more than 42% at the lowest range of the void fraction representing the bubbly and the unsteady pulsating flow regimes. The other notable observation is that the void fraction in last range is well predicted by the drift flux model of Dix (Woldesemayat and Ghajar [11]) with an extremely high prediction accuracy of 98.3% within ±10%. Moreover, both the homogeneous model of Nishino and Yamazaki [25] and the slip flow model of Spedding

and Chen [37] have a good accuracy with predictions more than 93%. For the middle range of the void fraction, the top performing model is the slip flow model of Hamersma and Hait [39] with a prediction accuracy of 75% within ±20%. Therefore, it is necessary to improve the accuracy of the void fraction models in the first and second ranges.

The top performing models of Zivi [32] and Turner and Wallis [33] to predict the void fraction in the first range of $0 < \alpha \leq 0.2$ are based on the slip flow model. For the void fraction in the second range of $0.2 < \alpha \leq 0.5$, the top performing models of Hamersma and Hait [39], Lokhart and Martinelli [29] and Spedding and Chen [37] are also based on the slip flow model. Therefore, the slip flow model is considered here in developing a new prediction method for the void fraction in the coiled rectangular channel with further considering the effect of other main parameters on the two-phase flow phenomena and corresponding flow regimes observed in the present study. From the slip flow models for the void fractions in Table 5, it is can be found that the void fraction is function of the gas mass fraction, the ratio of the gas and liquid densities and the ratio of liquid and gas dynamic viscosities. The slip flow model for the void fraction can be expressed as follows:

$$\alpha = f\left(\frac{1-x}{x},\ \frac{\rho_G}{\rho_L},\ \frac{\mu_L}{\mu_G}\right) \tag{9}$$

The void fraction is a function of the mass fraction of the two phases in the air- water two-phase flow and the physical properties such as densities and dynamic viscosities of the two phases.

Taking the model of Spedding and Chen [37] here, figure 17 shows the experimental void fraction versus the ratio of the mass fractions of the liquid phase and the gas phase $[(1-x)/x]^{0.65}$ used in the model of Spedding and Chen [37] for the liquid superficial velocity from 0.098 m/s to 0.882 m/s. It can be seen the experimental void fraction is not only strongly related to the ratio of the mass fractions of the two phases but also strongly related to the liquid superficial velocity. It is noted that the model of Spedding and Chen [37] predicts 93.2% of the experimental data for the void fraction in the last range of $0.5 < \alpha \leq 1$. The void fraction could be considered as a function of the ratio of the mass fractions of the two phases for higher void fractions as shown in Figure 17. However, for the void fraction in the first two ranges, the void fraction is not only related to the ratio of the mass fractions of the two phases, but also related to the liquid superficial velocity as indicated in Figure 17 for the lower void fractions. This is the reason why the slip flow model has a high accuracy in the last range of void fraction for higher void fraction data and in other two ranges has a low accuracy. Therefore, it is reasonable to use the slip flow model to develop new models in this case.

6.2. Mechanisms and new models for the void fraction in the horizontal helically coiled channel

It should be noted here that the various ranges of the void fractions corresponding to different flow regimes which are critical in understanding the two-phase flow phenomena and characteristics as observed in the experiments. The lowest range of the void fraction

represents the bubbly flow and the unsteady pulsating flow regimes. The void fraction in the unsteady pulsating flow regime may relate to the ratio of superficial velocities of the two phases. Furthermore, the liquid phase in the unsteady pulsating flow regime is significantly affected by the gravity. In the bubble flow regime, the liquid phase is mainly controlled by the centrifugal force induced in the coiled channel, which is a strong function of the liquid superficial velocity. Therefore, in developing a new model to capture the effect of the liquid superficial velocity in the low void fraction ranges, the liquid Froude number defined as the ratio of the inertia force to the gravity force is introduced in the new models, accounting for the effects of the two forces on the void fraction data in the range of lower void fractions. Furthermore, the ratio of the gas and liquid superficial velocities is also significant in developing the new model as it represents the slip of the two phases in the flow.

Figure 18 shows the variation of the experimental void fraction versus the product of the gas and liquid superficial velocity ratio and the liquid Froude number $\left(\frac{U_{SG}}{U_{SL}}\right)\left(\frac{1}{\sqrt{Fr}}\right)$. It is can be seen that the void fraction is well correlated with the ratio of gas and liquid superficial velocity ratio and the liquid Froude number. This has confirmed the afore-going analysis of the phenomena related to the corresponding flow regimes in the coiled rectangular channel. A uniform format of the void fraction is thus proposed for the void fraction in the first two ranges as follows:

$$\alpha = c\left[\left(\frac{U_{SG}}{U_{SL}}\right)\left(\frac{1}{\sqrt{Fr}}\right)\right]^{0.5n} \tag{10}$$

where the liquid Froude number is defined as

$$Fr = \frac{U_{SL}^2}{gd_E} \tag{11}$$

Based on the present experimental data, for the void fraction in the range of $0 < \alpha \leq 0.2$, c = 0.041 and n = 2. For the void fraction in the range of $0.2 < \alpha \leq 0.5$, c = 0.23 and n = 0.4.

For the void fraction in the last range of higher void fraction values, the drift flux model of Dix (Woldesemayat and Ghajar [11]) is recommended to predict the void fraction according to the afore-going comparison results.

The prediction methods for the average void fractions include the new proposed slip flow models for lower void fractions and the existing drift flux model for higher void fracrions. In order to select the appropriate calculation methods in the three ranges of void fractions, the criterion is given correlated with the gas volumetric flow fraction range β and Froude number Fr also shown in the following equations:

For the void fraction in the range of $0 < \alpha \leq 0.2$ ($\beta < 0.72$ and $0 < Fr \cdot \beta^{-1} \leq 4$), the follow correlation is applicable:

$$\alpha = 0.041\left(\frac{U_{SG}}{U_{SL}}\right)\left(\frac{1}{Fr^{0.5}}\right) \tag{12}$$

For the void fraction in the range of $0.2 < \alpha \leq 0.5$ ($\beta < 0.72$ and $4 < Fr \cdot \beta^{-1} \leq 30$), the

following correlation is applicable:

$$\alpha = 0.23\left(\frac{U_{SG}}{U_{SL}}\right)^{0.2}\left(\frac{1}{Fr^{0.1}}\right) \tag{13}$$

For the void fraction in the range of $0.5 < \alpha \leq 1$ ($0.72 < \beta \leq 1$), the drift flux model of Dix (Woldesemayat and Ghajar [11]) is applicable:

$$\alpha = \frac{U_{SG}}{U_{SG}\left(1+\left(\frac{U_{SL}}{U_{SG}}\right)^{\left(\frac{\rho_G}{\rho_L}\right)^{0.1}}\right)+2.9\left[\frac{g\sigma\left(\rho_L-\rho_G\right)}{\rho_L^{\,2}}\right]^{0.25}} \tag{14}$$

The whole experimental data covering all four flow regimes are compared to these methods including the new proposed models and the recommended model of Dix (Woldesemayat and Ghajar [11]). Figure 19 shows the comparative results of the measured void fractions to the predicted void fractions in the diagram of the average void fraction versus the gas mass fraction. It can be seen that the predicted data capture the measure data trends quite well in the whole experimental ranges covering all the four flow regimes observed in the experiments. Especially at lower void fractions, the new predicted methods well capture the experimental data. Figure 20 shows the comparison of the predicted void fractions to the experimental void fractions. It seems that the methods predict the experimental data quite well. Table 9 indicates the statistical results of the comparisons according to the three void fraction ranges. The new proposed models have significantly

improved the predictions of the void fraction. For the void fraction in the range of $0 < \alpha \leq 0.2$, the new model captures 76% of the experimental data within ±30% and for the void fraction in the range of $0.2 < \alpha \leq 0.5$, the new model captures 90% of the experimental data within ±20%. The Dix (Woldesemayat and Ghajar [11]) model predicts 98.3% of the experimental data for the void fraction within ±10% in the void fraction range of $0.5 < \alpha \leq 1$ as it does. Overall, for the entire experimental data, the new proposed models and the recommended model of Dix (Woldesemayat and Ghajar [11]) have a good predictive capability to calculate the average void fraction for the horizontal helically coiled rectangular channel, capturing 92.8% of all experimental point data within ±30%.

It should be mentioned here that the new models are based on the effects of the limiting parameters corresponding to the relevant flow regimes. The models satisfactorily predict the experimental for the horizontal helically coiled rectangular channel. It is recommended that these models be further examined with new measured experimental data in such types of channels in future.

7. Conclusions

Experiments on the average void fractions and the corresponding flow regimes were simultaneously measured and observed with the QCV method and the high-speed video camera in the present study. Then, the measured void fraction data were compared to 32 selected void fraction models and correlations. Furthermore, new models have been proposed to predict the void fractions in the helically coiled rectangular channel for the low

range of void fractions. The following conclusions are obtained:

(1) Four main flow regimes were observed in the test helically coiled rectangular channel, i.e. the unsteady pulsating flow, the bubbly flow, the intermittent flow and the annular flow at the test conditions in this study.

(2) From the experimental results, it is obtained that the average void fraction are not only correlated with the flow regimes but also related to the gas and liquid superficial velocities. The average void fractions in unsteady pulsating flow, bubbly flow and intermittent flow are strongly affected by both the liquid and gas superficial velocities while the liquid superficial velocity has a significant effect in the annular flow regime.

(3) The predictive capability of 32 selected void fraction models and correlations is evaluated for three ranges of void fractions ($0 < \alpha \leq 0.2$; $0.2 < \alpha \leq 0.5$ and $0.5 < \alpha \leq 1$) with the corresponding error band (±30%, ±20% and ±10%). The analysis shows that in the first range all the correlations have a low accuracy with predictions less than 41.2% within ±30%. This may because the unsteady pulsating flow regime has never been considered in these correlations. For the second range of void fraction, the Hamersma and Hait model gives the best performance with a prediction of 75% of the entire data within ±20%. For the third range of void fraction, the top performance is given by the model of Dix (Woldesemayat and Ghajar [11]) with a prediction of 98% of the entire data within ±10%. Therefore, the model of Dix is recommended for predicting the void fraction in the range of $0.5 < \alpha \leq 1$ while for the ranges of $0 < \alpha \leq 0.2$; $0.2 < \alpha \leq 0.5$, no models and correlations are satisfactory.

(4) The mechanistic maps and models for horizontal two-phase flow in straight

channels do not work for the experimental flow regime transitions in the coiled channels due to the non-circular channel and secondary flow generated in the coiled channel. As a result, the corresponding void fraction models developed for straight circular tubes are not applicable for the horizontal helically coiled channel. However, effort should be made to develop mechanistic flow regime maps and models for coiled channels in future.

(5) Taking into consideration of the effect of the ratio of gas to the superficial liquid velocity and the Froude number on the void fraction, new models for the void fraction ranges of $0 < \alpha \leq 0.2$; $0.2 < \alpha \leq 0.5$ have been proposed and can predict the experimental data reasonably well. Combining with the recommended model of Dix, 92.8% of the experimental data points are predicted with these models within an acceptable accuracy. It is suggested that the recommended and proposed models be evaluated with extensive experimental data under various conditions in future.

(6) It is recommended to obtain extensive experimental data for various channel sizes and arrangements of coiled rectangular channels in future. Furthermore, effort should be made to develop a generalized prediction method for coiled channels under different pipe orientations and pipe geometries. The effects of pipe orientations and pipe geometries correlated with the average void fraction data are suggested as the future work.

Acknowledgement

This research is founded by the National Natural Science Foundation of China (No. 51576005).

Nomenclature

A_R	rectangular cross-section area, m^2
C_0	the distribution parameter
D	coil diameter, m
d_E	equivalent diameter, m
G	mass flux, kg/m^2s
g	gravity acceleration, m/s^2
h	channel height, m
P	pitch, m
U_{gm}	drift velocity, m/s
U_M	mixture velocity, m/s
U_{SG}	superficial gas velocity, m/s
U_{SL}	superficial liquid velocity, m/s
V	the volume of liquid phase filled in the test section, m^3
V_i	liquid volume of two-phase flow remaining in the test section, m^3

Greek letters

α	channel average void fraction
β	homogeneous volume fraction
θ	the round angle from the channel inlet

ρ	density
μ	kinetic viscosity

Subscript

E	equivalent
R	rectangular cross-section
SG	gas superficial
SL	liquid superficial

Dimensionless number

Fr	Froude number

Abbreviation

QCV	quick-closing valve method

References

[1] A.K. Thandlam, T.K. Mandal, S.K. Majumder, Flow pattern transition, frictional pressure drop, and holdup of gas non-Newtonian fluid flow in helical tube, ASIA-Pacific J. Chem. Eng. 10, (2015) 422–437.

[2] Y. Murai, S. Yoshikawa, S.I. Toda, M.A. Ishikawa, F. Yamamoto, Structure of air–water two-phase flow in helically coiled tubes, Nucl. Eng. Des. 236, (2006) 94–106.

[3] H.Y. Zhu, Z.X. Li, X.T. Yang, G.Y. Zhu, J.Y. Tu, S.Y. Jiang, Flow regime identification for upward two-phase flow in helically coiled tubes, Chem. Eng. J. 308 (2017) 606-618.

[4] S. Banerjee, E. Rhodes, D.S. Scott, Studies on co-current gas-liquid flow in helically coiled tubes. I. Flow patterns, pressure drop and holdup, Can. J. Chem. Eng. 47 (1969) 445–453.

[5] L. Cheng, G. Ribatski, J.R. Thome, Gas-liquid two-phase flow patterns and flow pattern maps: Fundamentals and Applications, ASME. Appl. Mech. Rev. 61 (2008) 050802.

[6] R. Srisomba, O. Mahian, A.S. Dalkilic, S. Wongwises, Measurement of the void fraction of R-134a flowing through a horizontal tube, Int. Comm. Heat Mass Transfer 56 (2014) 8-14.

[7] S.P. Oliviera, J.P. Meyera, M.D. Paepe, K.D. Kerpel. The influence of inclination angle on void fraction and heat transfer during condensation inside a smooth tube, Int. J. Multiphase Flow 80 (2016) 1-14

[8] V. Jagan, A. Satheesh. Experimental studies on two-phase flow patterns of air-water mixture in a pipe with different orientations. Flow Meas. Instrum. 52 (2016) 170-179.

[9] J.A. Milkie, S. Garimella，M. P. Macdonald, Flow regimes and void fractions during condensation of hydrocarbons in horizontal smooth tubes, Int. J. Heat Mass Transfer 92 (2016) 252-267

[10] M. Lockanathan, T. Hibiki, Flow regime, void fraction and interfacial area transport and characteristics of co-current downward two-phase flow, Nuclear Eng. Des. 307 (2016) 39-63

[11] M.A. Woldesemayat, A.J. Ghajar, Comparison of void fraction correlations for different flow patterns in horizontal and upward inclined pipes, Int. J. Multiphase Flow 33 (2007) 347-370.

[12] Y.Q. Xue, H.X. Li, C.Y. Hao, C. Yao, Investigation on the void fraction of gas-liquid two-phase flows in vertically-downward pipes, Int. Comm. Heat and Mass Transfer 77 (2016) 1-8.

[13] S.N. Mandal, S. K. Das, Gas–liquid flow through helical coils in horizontal orientation, Can. J. Chem. Eng. 80 (2002) 979-983

[14] A.B. Biswas, S.K. Das, Two-phase frictional pressure drop of gas-non-Newtonian liquid flow through helical coils in vertical orientation, Chem. Eng. Prog. 47 (2008) 816–826.

[15] X.F. Liu, D.H. Zhao, Y.F. Liu, S. Jiang, H.Z. Xiang. Numerical analysis of the two-phase flow characteristics in vertical downward helical pipe. Int. J. Heat Mass Transfer 108 (2017) 1947–1959.

[16] G.D. Xia, X.F. Liu, An investigation of two-phase flow pressure drop in helical rectangular channel, Int. Commun. Heat Mass Transfer 54 (2014) 33-41.

[17] G.D. Xia, X.F. Liu, Y.L. Zhai, Z.Z. Cui, Single-phase and two-phase flows through helical channels in single screw expander prototype, J. Hydrodyn. Ser. B 26 (2014) 114–121.

[18] L. Cheng, G. Ribatski, L. Wojtan, J.R. Thome, New flow boiling heat transfer model and flow pattern map for carbon dioxide evaporation inside horizontal tubes, Int. J. Heat Mass Transfer 49 (2006) 4082-4094.

[19] L. Cheng, G. Ribatski, J. Moreno Quibén, J.R. Thome, New prediction methods for CO_2 evaporation inside tubes: Part I—A two-phase flow pattern map and a flow pattern based phenomenological model for two-phase flow frictional pressure drops, Int. J. Heat Mass Transfer 51 (2008) 111-124.

[20] L. Cheng, G. Ribatski, J.R. Thome, New prediction methods for CO_2 evaporation inside tubes: Part II - An updated general flow boiling heat transfer model based on flow patterns, Int. J. Heat Mass Transfer 51 (2008) 125-135.

[21] J. Moreno Quibén, L. Cheng, R.J. da Silva Lima, J.R. Thome, Flow boiling in horizontal flattened tubes: Part I — two-phase frictional pressure drop results and model, Int. J. Heat Mass Transfer 52 (2009) 3634-3644.

[22] J. Moreno Quibén, L. Cheng, R.J. da Silva Lima, J.R. Thome, Flow boiling in horizontal flattened tubes: Part II — Flow boiling heat transfer results and model, Int. J. Heat Mass Transfer 52 (2009) 3645-3653.

[23] J.R. Taylor, An Introduction to Error Analysis, second ed., University Science Books, 1997.

[24] A.J. Ghajar, S.M. Bhagwat. Effect of void fraction and two-phase dynamic viscosity models on prediction of hydrostatic and frictional pressure drop in vertical upward gas-liquid two phase flow. Heat Transfer Eng. 34 (13) (2013) 1044-1059

[25] H. Nishino, Y. Yamazaki, A new method of evaluating steam volume fractions in boiling systems, Journal- Atomic Energy Society of Japan 5 (1963) 39-46.

[26] A.L. Guzhov, V.A. Mamayev, G.E. Odishariya, A study of transportation in gas liquid systems, 10th International Gas Union Conference, Hamburg, Germany, 1967.

[27] D. Chisholm, Pressure gradients due to friction during the flow of evaporating two-phase mixtures in smooth tubes and channels, Int. J. Heat Mass Transfer 16(2) (1973) 347-358.

[28] V. Czop, D. Barbier, S. Dong, Pressure drop, void fraction and shear stress measurements in an adiabatic two-phase flow in a coiled tube, Nucl. Eng. Des. 149 (1-3) (1994) 323-333

[29] R.W. Lockhart, R.C. Martinelli, Proposed correlation of data for isothermal two-phase, two component flow in pipes. Chem. Eng. Progr. 45 (1949) 39-48.

[30] H. Fauske, Critical two-phase, steam–water flows. In: Proceedings of the 1961 Heat Transfer and Fluid Mechanics Institute. Stanford University Press, Stanford, CA, pp. 79–89. 1961.

[31] J.R.S. Thom, Prediction of pressure drop during forced circulation boiling of water, Int. J. Heat Mass Transfer 7 (7) (1964) 709-724.

[32] S. Zivi, Estimation of steady-state steam void-fraction by means of the principle of minimum entropy production, J. Heat Transfer 86(2) (1964) 247-251.

[33] J.M. Turner, G.B. Wallis, The separate-cylinders model of two-phase flow. Paper No. NYO-3114-6. Thayer's School Eng., Dartmouth College, Hanover, NH, USA. 1965

[34] C.J. Baroczy, A systemic correlation for two phase pressure drop, Chem. Eng. Progr. Symp. Ser. 62 (1966) 232-249.

[35] S.L. Smith, Void fractions in two phase flow: a correlation based upon an equal velocity head model. Proc. Inst. Mech. Engrs, London 184 (1969), 647–657, Part 1.

[36] X.F. Liu, D.H. Zhao, Y.F. Liu, S. Jiang, H.Z. Xiang. Numerical analysis of the

two-phase flow characteristics in vertical downward helical pipe. Int. J. Heat Mass Transfer 108 (2017) 1947–1959.

[37] P.L. Spedding, J.J.J. Chen, Holdup in two phase flow, Int. J. Multiphase Flow 10(3) (1984) 307-339.

[38] J.J.J Chen, A further examination of void-fraction in annular two-phase flow. Int. J. Heat Mass Transfer 29 (1986) 1760-1763.

[39] P. J. Hamersma, J. Hait, A pressure drop correlation for gas/liquid pipe flow with a small liquid holdup, Chem. Eng. Sci. 42 (5) (1987) 1187-1196.

[40] D.J. Nicklin, J.O. Wilkes, J.F. Davidson, Two-phase flow in vertical tubes, Trans. Instn. Chem. Engrs. 40 (1962) 61–68.

[41] S.Z. Rouhani, E. Axelsson, Calculation of void volume fraction in the subcooled and quality boiling regions, Int. J. Heat Mass Transfer 13 (2) (1970) 383-393.

[42] R.H. Bonnecaze, W. Erskine, E.J. Greskovich, Holdup and pressure drop for two phase slug flow in inclined pipes, AIChE J. 17 (1971) 1109-1113.

[43] E.J. Greskovich, W.T. Cooper, Correlation and prediction of gas-liquid holdups in inclined upflows, AICHE J. 21(6) (1975) 1189-1192.

[44] K.H. Sun, R.B. Duffey, C.M. Peng, A thermal-hydraulic analysis of core uncovery. In: Proceedings of the 19th National Heat Transfer Conference, Experimental and Analytical Modelling of LWR Safety Experiments, Orlando, Florida, July 27–30 (1980) 1-10.

[45] D. Jowitt, C.A. Cooper, K.G. Pearson, The thetis 80 % blocked cluster experiments part 5: level swell experiments safety and engineering science, 1984

[46] D. Bestion, The Physical closure laws in the CATHARE code. Nucl. Eng. Des. 124 (1990) 229-245

[47] L, Mattar, G.A. Gregory. Air oil slug flow in an upward-inclined pipe – I: Slug velocity, holdup and pressure gradient. J. Can. Petroleum Technol. 13 (1974) 69–76.

[48] K. Mishima, T. Hibiki, Some characteristics of air-water two-phase flow in small diameter vertical tubes, Int. J. Multiphase Flow 22 (4) (1996) 703-712.

[49] J. Hart, P.J. Hamersma, J.M.H. Fortuin, Correlations predicting frictional pressure drop and liquid holdup during horizontal gas-liquid pipe flow with a small liquid holdup. Int. J. Multiphase Flow 15 (1989) 947-964.

[50] R.H. Huq, J.L. Loth, Analytical two-phase flow void fraction prediction method. J. Thermo Phys. 6 (1992) 139–144.

[51] L.G. Neal, S.G. Bankoff, Local parameters in co-current mercury–nitrogen flow: Parts I and II, AIChE J. 11 (1965) 624–635.

[52] A. Cioncoloni, J.R. Thome, Void Fraction Prediction in Annular Two Phase Flow. Int. J. Multiphase Flow 43 (2012) 72-84.

[53] Y. Taitel, A.E. Dukler, A model for predicting flow regime transitions in horizontal and near horizontal gas-liquid flow, AIChE J. 22 (1976) 47–55.

[54] Y. Taitel, D. Bornea, A.E. Dukler, Modelling flow pattern transitions for steady upward gas-liquid flow in vertical tubes, AIChE J. 26 (1980) 345–354

[55] H. Q. Zhang, Q. Wang, C. Sarica, J. P. Brill. Unified Model for Gas-Liquid Pipe Flow via Slug Dynamics—Part 1: Model Development. ASME J. Energy Res. Technol. 125 (2003) 266-273.

[56] H. Q. Zhang, Q. Wang, C. Sarica, J. P. Brill. Unified Model for Gas-Liquid Pipe Flow via Slug Dynamics—Part 2: Model Validation. ASME J. Energy Res. Technol. 125 (2003) 274-283.

[57] H. Q. Zhang, Q. Wang, C. Sarica, J. P. Brill. A unified mechanistic model for slug liquid holdup and transition between slug and dispersed bubble flows. Int. J. Multiphase Flow 29 (2003) 97–107.

List of Table Captions

List of Figure Captions

Fig. 16. Variation of the experimental void fraction with the dimensionless parameter $[(1-x)/x]^{0.65}$.

Fig. 17. Variation of the experimental void fraction with the dimensionless parameter of $(U_{SG}/U_{SL})/Fr^{0.5}$.

Fig. 18. Variation of the measured average void fraction and the predicted void fraction with the gas mass fraction.

Fig. 19. Comparative results of the measured void fraction to the predicted void fraction with the new proposed models for void fraction the first and second void fraction ranges of $0 < \alpha \leq 0.2$ and $0.2 < \alpha \leq 0.5$ and the recommended model for the void fraction in the range of $0.5 < \alpha \leq 1$.

Table 1. Geometry parameters of the helical coiled rectangular channel.

Parameters	Value
Channel height, h (m)	0.034
Channel width, w (m)	0.025
Pitch, P (m)	0.140
Coil diameter, D (m)	0.141
Helix angle, φ (°)	**17.5**

Table 2 The types, modes and manufactures of the instrument/equipment.

Instrument/equipment	Type/mode	Types and Manufactures
Centrifugal pump	CHL2	Nanfang Pump Industry, China
Electromagnetic flow meter	GHLDG-25	Tianjin Flow Meter, China
Air screw compressor	SA45A	Beijing Fucheng Machinery, China
Gas flow meter	HS-6000	Beijing Heshi, Automation Technology China
Solenoid valve	2W-25	Beijing Heshi, Automation Technology, China
High-speed camera	Motion Pro X4	Redlake, America
Data acquisition unit	34972A	Agilent, America

Table 3 Experimental conditions and uncertainties of the measured parameters.

Parameter	Range	Unit	Uncertainties
Area of channel A_R	-	m^2	±1.18%
Superficial liquid velocity U_{SL}	0.11 ~ 2	m/s	±3.22%
Superficial gas velocity U_{SG}	0.18 ~ 16	m/s	±5.99%
Averagemod void fraction $<\alpha>$	0.012 ~ 0.927	-	±2.8%

Table 4. The homogeneous flow models for the void fraction.

Author	The void fraction model
Armand [a]	$\alpha = 0.833\alpha_{\mathrm{H}}$
Nishino and Yamazaki [25]	$\alpha = 1-\left(\frac{1-x}{x}\frac{\rho_G}{\rho_L}\alpha_{\mathrm{H}}\right)^{0.5}$
Guzhov et al. [26]	$\alpha = 0.81\alpha_{\mathrm{H}}\left[1-\exp\left(-2.2\sqrt{Fr}\right)\right]$
Chisholm [27]	$\alpha = \frac{\alpha_{\mathrm{H}}}{\alpha_{\mathrm{H}}+\left(1-\alpha_{\mathrm{H}}\right)^{0.5}}$
Cozp et al. [28]	$\alpha = -0.285+1.097\alpha_{\mathrm{H}}$

[a] Reported by Woldsemayat and Ghajar [11]

Table 5. The slip flow models for the void fraction.

Author	The void fraction model
Lockhart and Martinelli [29]	$\alpha = \left[1+0.28\left(\frac{1-x}{x}\right)^{0.64}\left(\frac{\rho_G}{\rho_L}\right)^{0.36}\left(\frac{\mu_L}{\mu_G}\right)^{0.07}\right]^{-1}$
Fauske [30]	$\alpha = \left[1+\left(\frac{1-x}{x}\right)\left(\frac{\rho_G}{\rho_L}\right)^{0.5}\right]^{-1}$
Thom [31]	$\alpha = \left[1+\left(\frac{1-x}{x}\right)\left(\frac{\rho_G}{\rho_L}\right)^{0.89}\left(\frac{\mu_L}{\mu_G}\right)^{0.18}\right]^{-1}$
Zivi [32]	$\alpha = \left[1+\left(\frac{1-x}{x}\right)\left(\frac{\rho_G}{\rho_L}\right)^{0.67}\right]^{-1}$
Turner and Wallis [33]	$\alpha = \left[1+\left(\frac{1-x}{x}\right)^{0.72}\left(\frac{\rho_G}{\rho_L}\right)^{0.4}\left(\frac{\mu_L}{\mu_G}\right)^{0.08}\right]^{-1}$
Baroczy [34]	$\alpha = \left[1+\left(\frac{1-x}{x}\right)^{0.74}\left(\frac{\rho_G}{\rho_L}\right)^{0.65}\left(\frac{\mu_L}{\mu_G}\right)^{0.13}\right]^{-1}$
Smith [35]	$\alpha = \left[1+A_S\left(\frac{1-x}{x}\right)\left(\frac{\rho_G}{\rho_L}\right)\right]^{-1}$ $A_S = 0.4+0.6\sqrt{\left[\frac{\rho_L}{\rho_G}+0.4\left(\frac{1-x}{x}\right)\right]/\left[1+0.4\left(\frac{1-x}{x}\right)\right]}$
Chisholm [27]	$\alpha = \left[1+A_S\left(\frac{1-x}{x}\right)\left(\frac{\rho_G}{\rho_L}\right)\right]^{-1}$ $A_S = \sqrt{1-x\left(1-\frac{\rho_L}{\rho_G}\right)}$
Spedding and Chen [37]	$\alpha = \left[1+2.22\left(\frac{1-x}{x}\right)^{0.65}\left(\frac{\rho_G}{\rho_L}\right)^{0.65}\right]^{-1}$
Chen [38]	$\alpha = \left[1+0.18\left(\frac{1-x}{x}\right)^{0.6}\left(\frac{\rho_G}{\rho_L}\right)^{0.33}\left(\frac{\mu_L}{\mu_G}\right)^{0.07}\right]^{-1}$
Hamersma and Hart [39]	$\alpha = \left[1+0.26\left(\frac{1-x}{x}\right)^{0.67}\left(\frac{\rho_G}{\rho_L}\right)^{0.33}\right]^{-1}$

Table 6. The drift flux models for the void fraction.

Author	The void fraction model
Nicklin et al. [40]	$\alpha = \frac{U_{SG}}{1.2U_M + 0.35\sqrt{gd}}$
Rouhani and Axelsson [41]	$C_0 = 1 + 0.2(1-x)\left(gd\rho_L^2/G^2\right)^{0.25}$ $(for\ \alpha \le 0.1)$ $C_0 = 1 + 0.2(1-x)$ $(for\ \alpha \ge 0.1)$ $U_{gm} = 1.18\left[\frac{g\sigma(\rho_L - \rho_G)}{\rho_L^2}\right]^{0.25}$
Bonnecaze et al. [42]	$C_0 = 1.2,\ U_{gm} = 0.35\sqrt{gd}\left(1 - \frac{\rho_G}{\rho_L}\right)$
Greskovich and Cooper [43]	$C_0 = \left(0.82 + 0.18\,P_{sys}/P_{crit}\right)^{-1},\ U_{gm} = 0.671\sqrt{gD}\left(\sin\theta\right)^{0.263}$
Sun et al. [44]	$C_0 = \left(0.82 + 0.18\,P_{sys}/P_{crit}\right)^{-1},\ U_{gm} = 1.41\left[\frac{g\sigma(\rho_L - \rho_G)}{\rho_L^2}\right]^{0.25}$
Dix [a]	$C_0 = \frac{U_{SG}}{U_{SG} + U_{SL}}\left(1 + \left(\frac{U_{SL}}{U_{SG}}\right)^{\left(\frac{\rho_G}{\rho_L}\right)^{0.1}}\right),\quad U_{gm} = 2.9\left[\frac{g\sigma(\rho_L - \rho_G)}{{\rho_L}^2}\right]^{0.25}$
Toshiba [a]	$\alpha = \frac{U_{SG}}{1.08U_M + 0.45}$
Jowitt et al. [45]	$C_0 = 1 + 0.796\exp\left(-0.061\sqrt{\frac{\rho_L}{\rho_G}}\right),\ U_{gm} = 0.034\left(\sqrt{\frac{\rho_L}{\rho_G}} - 1\right)$
Bestion [46]	$C_0 = 1,\ U_{gm} = 0.188\sqrt{\frac{gd(\rho_L - \rho_G)}{\rho_G}}$
Mattar and Gregory [47]	$C_0 = 1.3,\ U_{gm} = 0.7$
Mishima and Hibiki [48]	$C_0 = 1.2 + 0.51\exp\left(-0.691d\right),\ U_{gm} = 0$
Woldesemayat and Ghajar [11]	$C_0 = \frac{U_{SG}}{U_{SG} + U_{SL}}\left(1 + \left(\frac{U_{SL}}{U_{SG}}\right)^{\left(\frac{\rho_G}{\rho_L}\right)^{0.1}}\right),$ $U_{gm} = 2.9\left[\frac{gd\sigma(1+\cos\theta)(\rho_L - \rho_G)}{{\rho_L}^2}\right]^{0.25}\left(1.22 + 1.22\sin\theta\right)^{\frac{P_{atm}}{P_{system}}}$

[a] Reported by Woldesemayat and Ghajar [11]

Table 7. Other empirical void fraction correlations.

Author	The void fraction correlation
Hart et al. [49]	$\alpha = \left\{1+\frac{U_{SL}}{U_{SG}}\left[1+\left(108\,\mathrm{Re}_L^{-0.726}\frac{\rho_L}{\rho_G}\right)^{0.5}\right]\right\}^{-1}$
Huq and Loth [50]	$\alpha = 1-\frac{2(1-x)^2}{1-2x+\left[1+4x(1-x)\left(\frac{\rho_L}{\rho_G}-1\right)\right]^{0.5}}$
Neal and Bankoff [51]	$\alpha = 1.25\left(\frac{U_{SG}}{U_M}\right)^{1.88}\left(\frac{U_{SL}^2}{gd}\right)^{0.2}$
Cioncoloni and Thome [52]	$\alpha = \frac{hx^n}{1+(h-1)x^n}$ Where, $h = -2.129+3.129\left(\rho_g\rho_l^{-1}\right)^{-0.2186}$ and $n = 0.3487+0.6513\left(\rho_g\rho_l^{-1}\right)^{0.5150}$

Table 8. The best three models and correlations for the measured void fractions in the horizontal helically coiled rectangular channel.

Void fraction Range $0 < \alpha \leq 0.2$	Error ±30%	Void fraction Range $0.2 < \alpha \leq 0.5$	Error ±20%	Void fraction Range $0.5 < \alpha \leq 1$	Error ±10%
Homogeneous model					
Czop et al. [28]	17.6	Nishino and Yamazaki [25]	55	Nishino Yamazaki [25]	93.2
-	-	Czop et al. [28]	30	Czop et al. [28]	83.1
-	-	Chisholm [27]	25	Chisholm [27]	76.3
Slip flow model					
Zivi [32]	41.2	Hamersma and Hait [39]	75	Spedding and Chen [37]	93.2
Turner and wallis [33]	41.2	Lokhart and Martinelli [29]	65	Chen [38]	88.1
Thom [31]	23.5	Spedding and Chen [37]	60	Smith [35]	81.4
Drift flux model					
Bestion [46]	23.5	Mishima and Hibiki[48]	60	Dix [a]	98.3
-	-	Mattar and Gregory [47]	55	Jowitt et al. [45]	79.7
-	-	Jowitt et al. [45]	35	Rouhani and Axelsson [41]	79.7
Other empirical correlations					
Hart et al. [49]	29.4	Huq and Loth [50]	40	Huq and Loth [50]	88.1
Neal and Bankoff [51]	11.8	Neal and Bankoff[51]	15	Cioncoloni and Thome [52]	78.0
-	-	Hart et al. [49]	5	Hart et al. [49]	35.6

[a] Reported by Woldesemayat and Ghajar [11]

Table 9. The statistical results of the new proposed and recommended models compared to the measured void fraction data.

Void fraction Range	Error band	Data points within error band
$0 < \alpha \leq 0.2$	±30%	76%
$0.2 < \alpha \leq 0.5$	±20%	90%
$0.5 < \alpha \leq 1$	±10%	98%
$0 < \alpha \leq 1$	±30%	92.8%

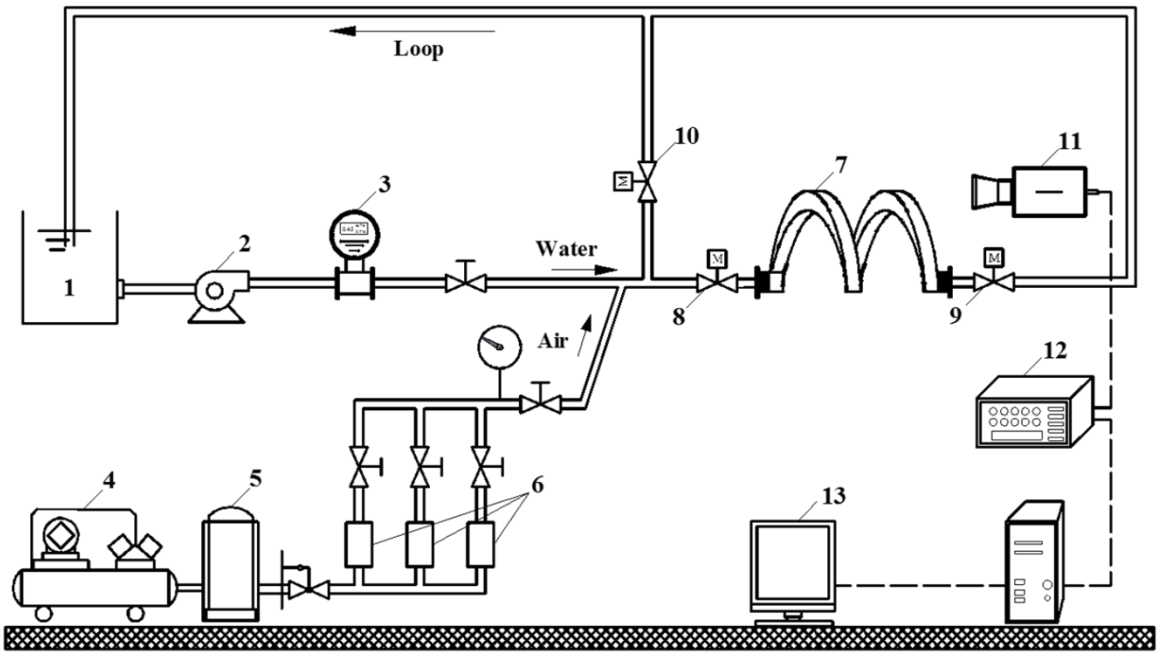

Fig. 1. Schematic diagram of the experimental setup for air-water two-phase flow for the measurement of the void fraction.

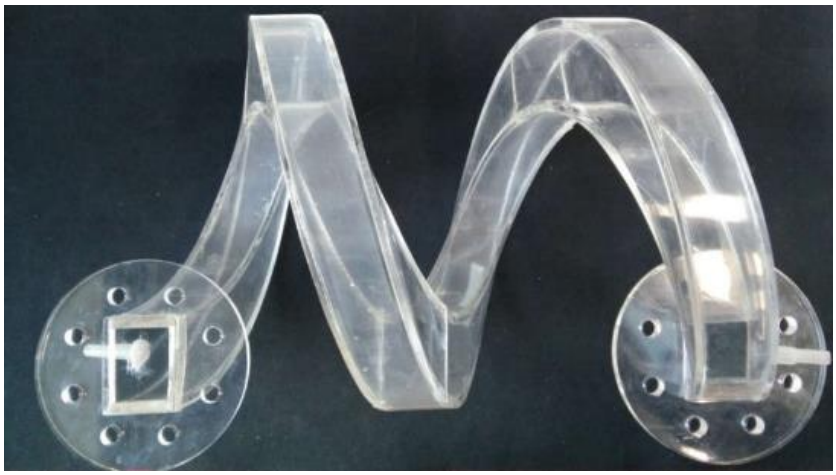

Fig. 2. Photography of the test section.

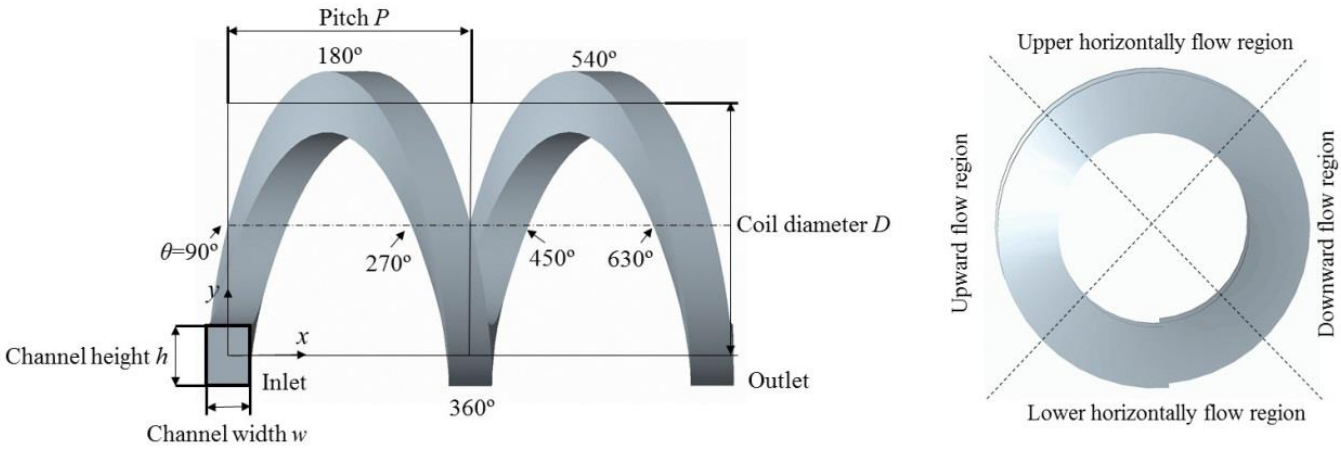

Fig. 3. Schematic diagram of the helically coiled rectangular channel and its geometry dimensions.

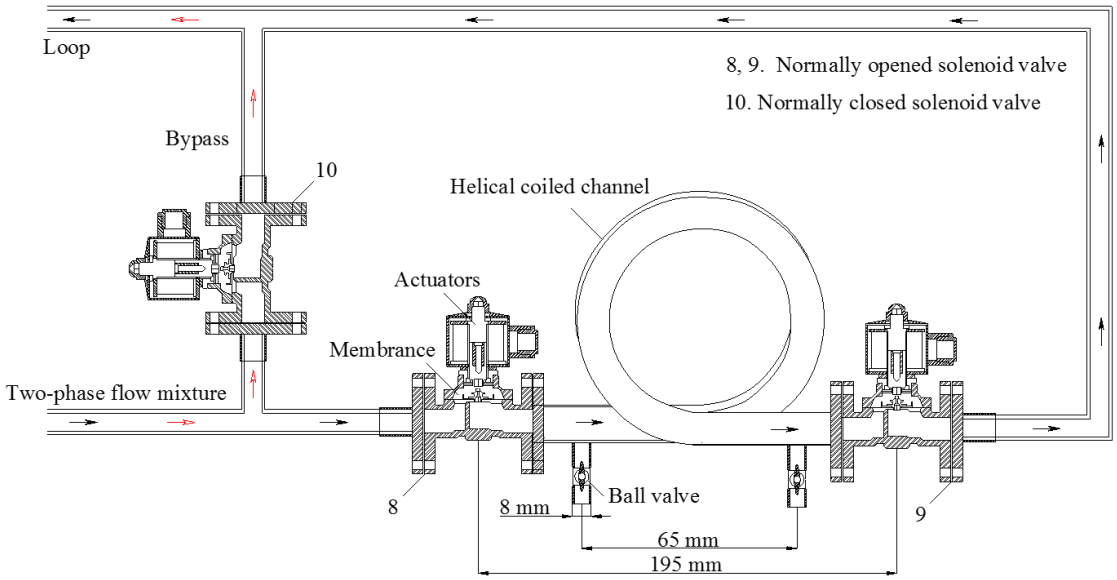

Fig. 4. Schematic diagram of the quick-closing (QCV) method for measuring the average void fraction in the test channel.

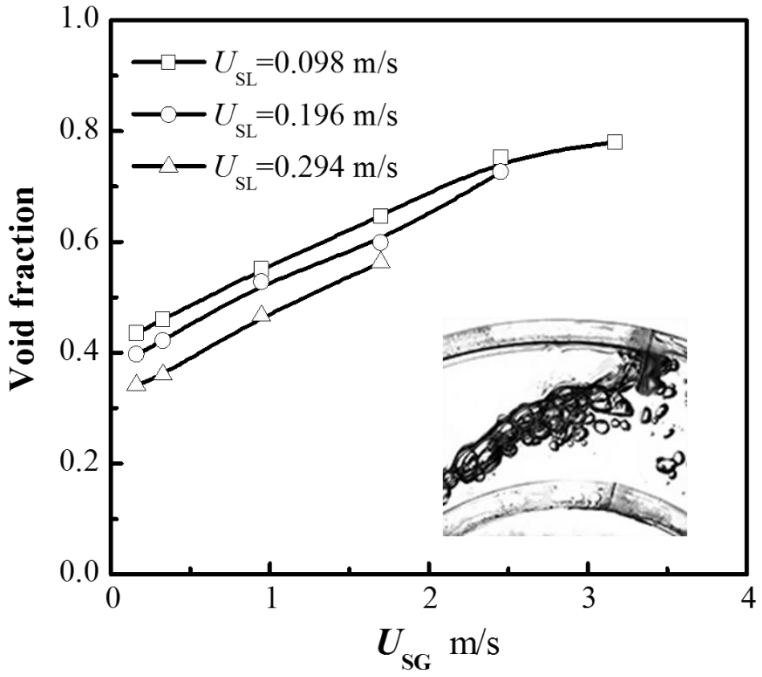

Fig. 5. The measured average void fractions for the unsteady pulsating flow regime.

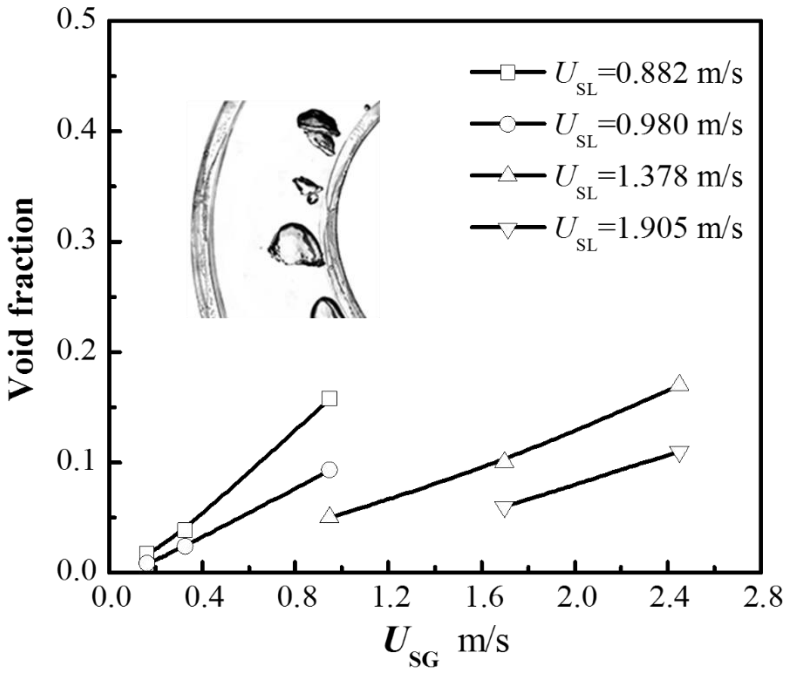

Fig. 6. The measured average void fractions for the bubbly flow regime.

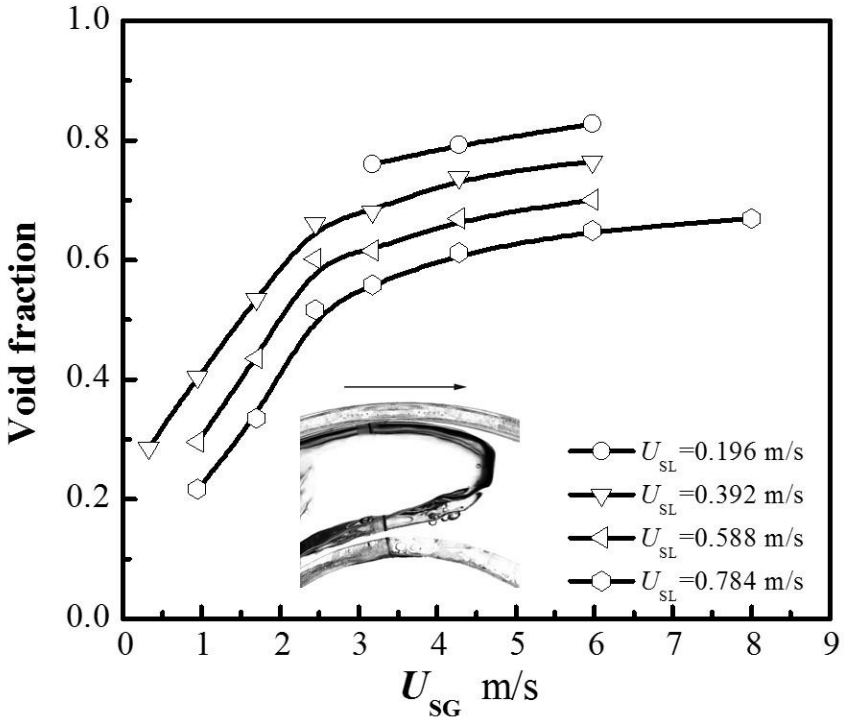

Fig. 7. The measured average void fractions for the intermittent flow regime.

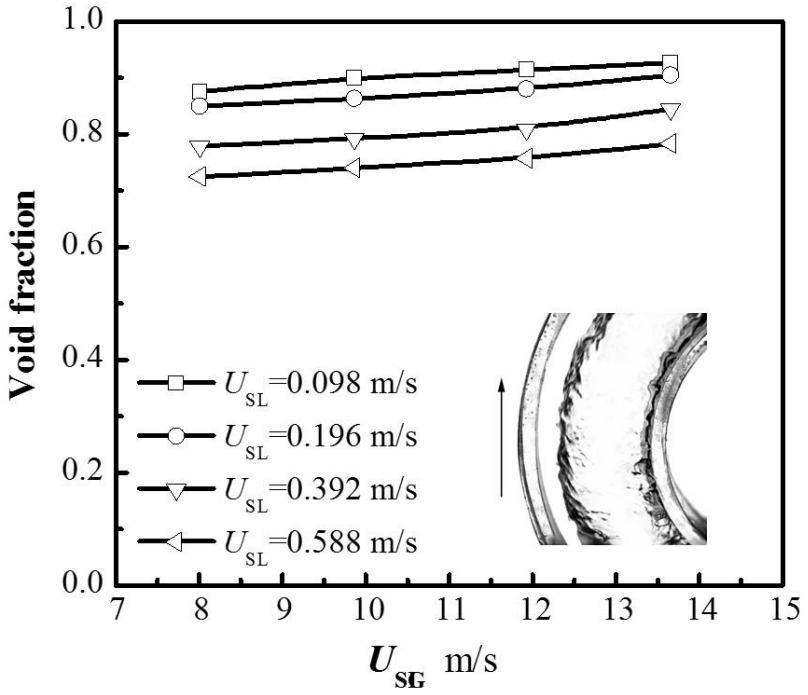

Fig. 8. The measured average void fractions for the annular flow regime.

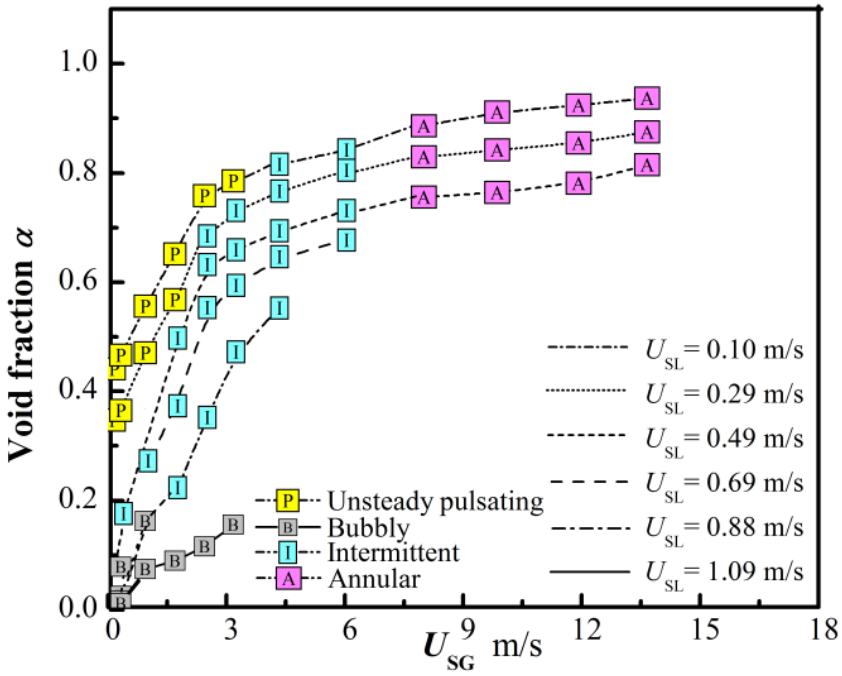

Fig. 9. Comparison of the measured average void fractions at various conditions for the four flow regimes.

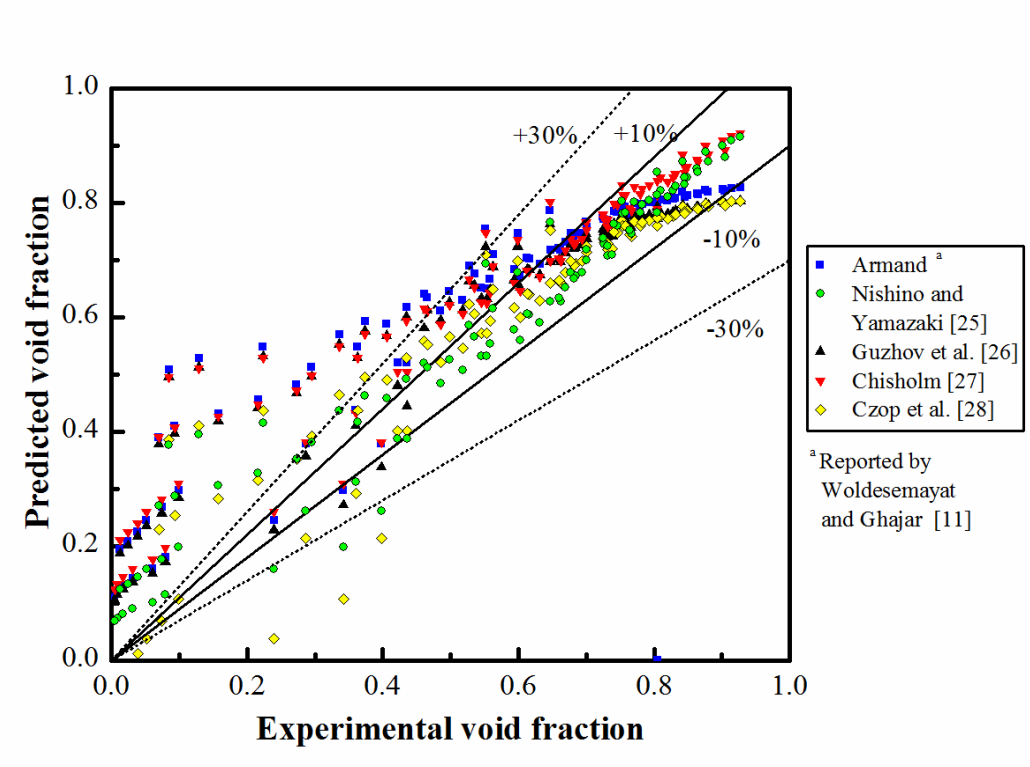

Fig. 10. Comparative results of the measured void fractions to the predicted void fractions with the homogeneous models.

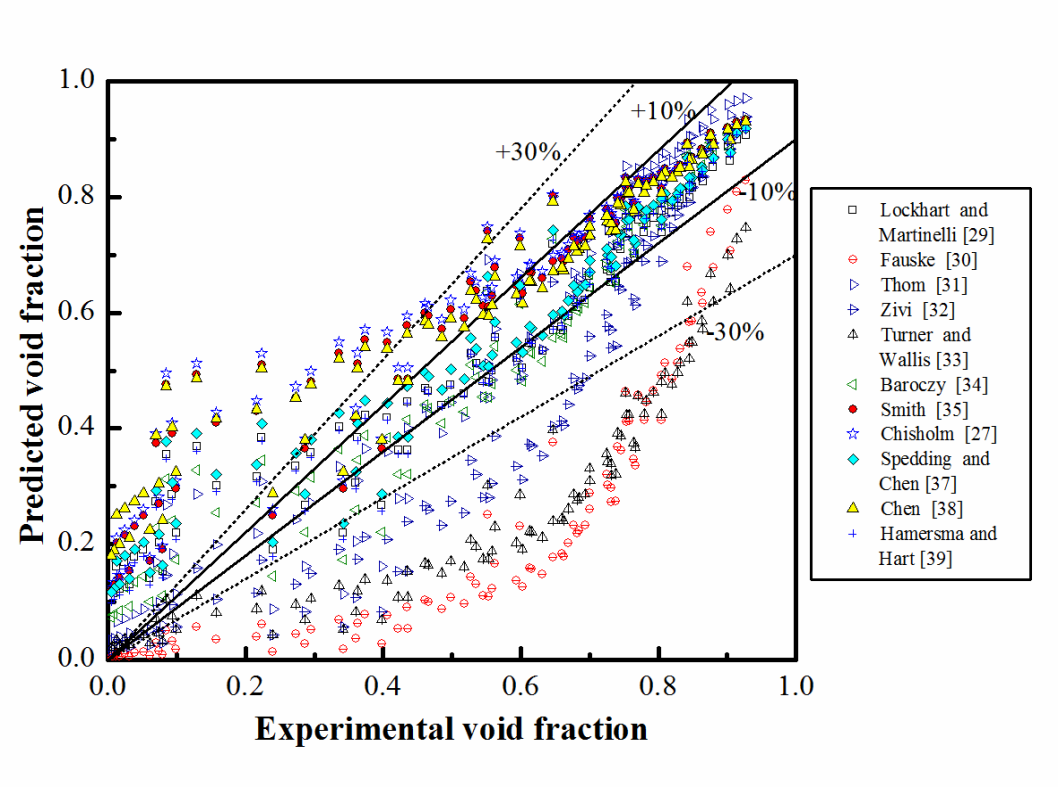

Fig. 11. Comparative results of the measured void fractions to the predicted void fractions with the slip flow models.

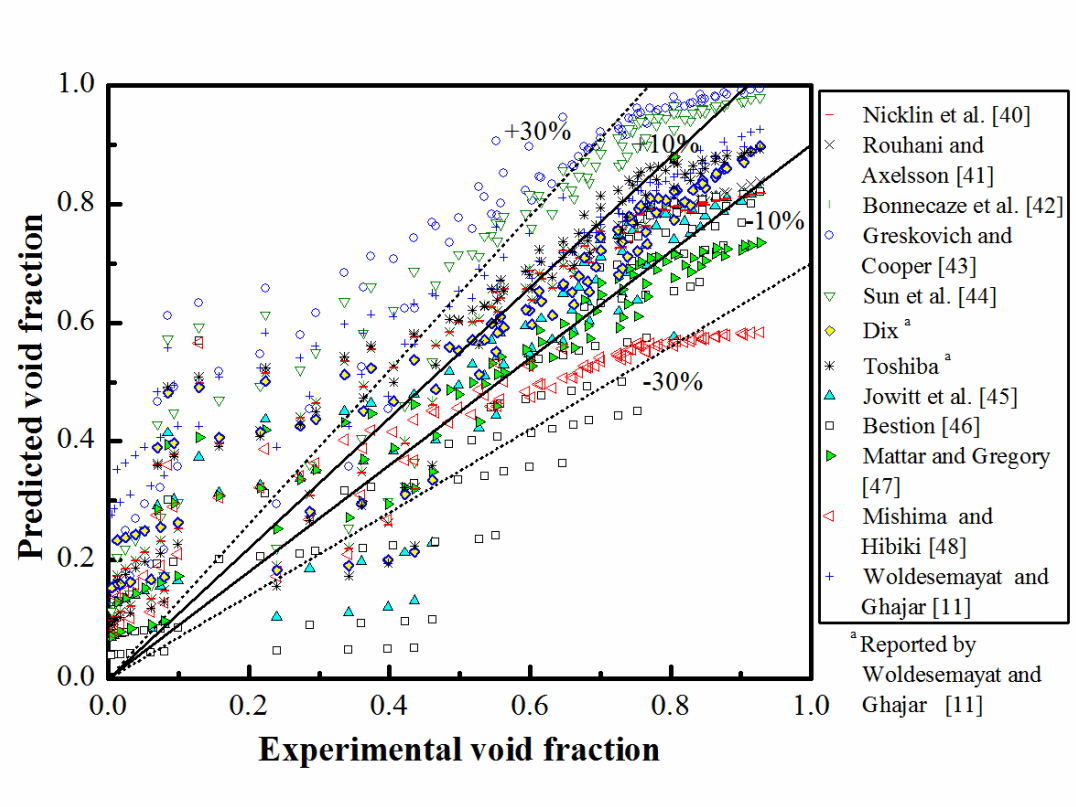

Fig. 12. Comparative results of the measured void fractions to the predicted void fractions with the drift flux models.

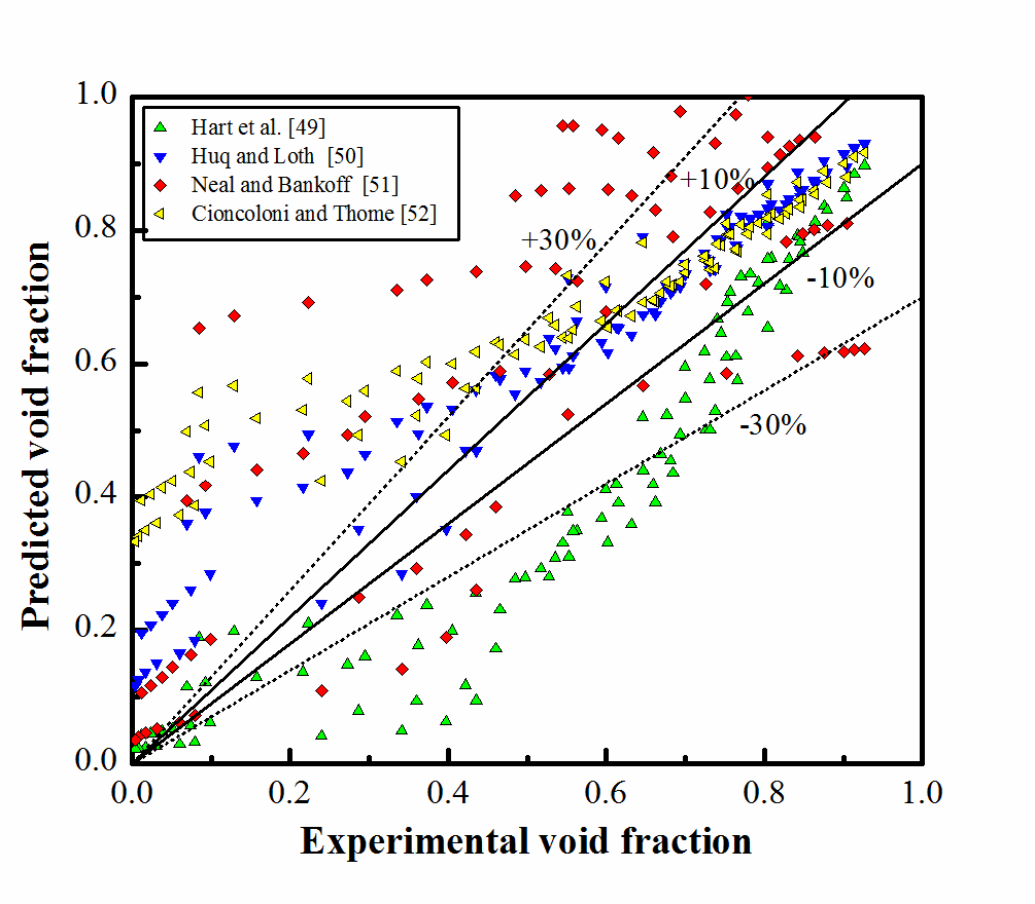

Fig. 13. Comparative results of the measured void fractions to the predicted void fractions with other empirical correlations.

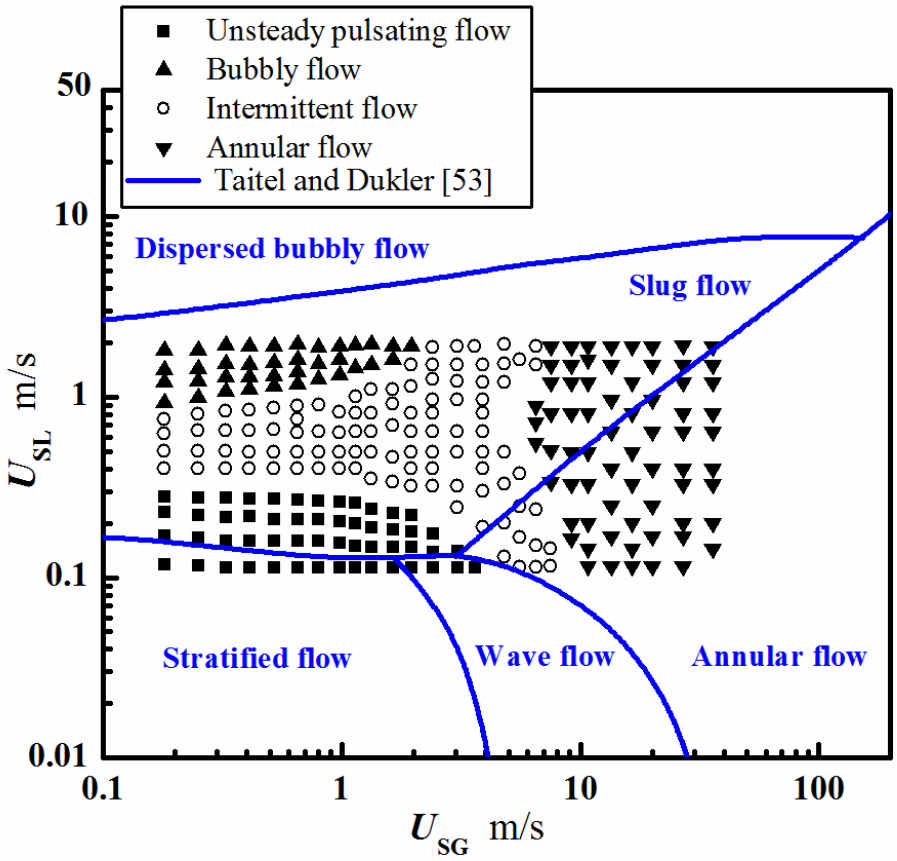

Fig.14. Comparison of experimental flow regimes to the mechanistic flow model and map of Taitel and Dukler [53] horizontal two-phase flow.

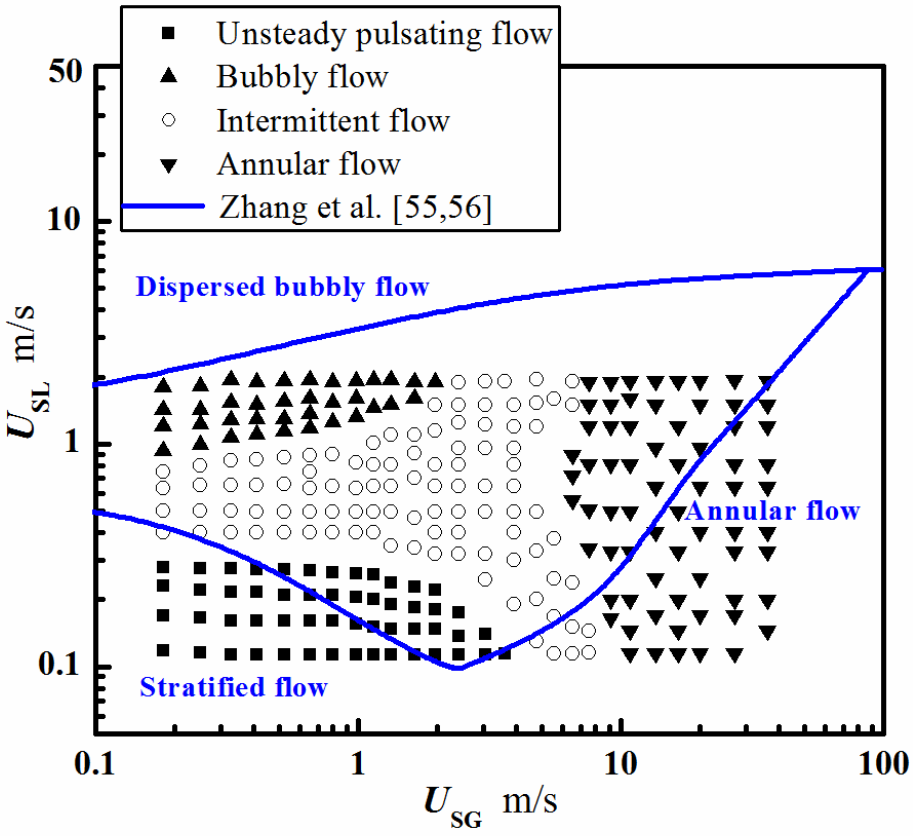

Fig. 15. Comparison of experimental flow regimes to the mechanistic flow model and map of Zhang et al [55, 56] for horizontal two-phase flow.

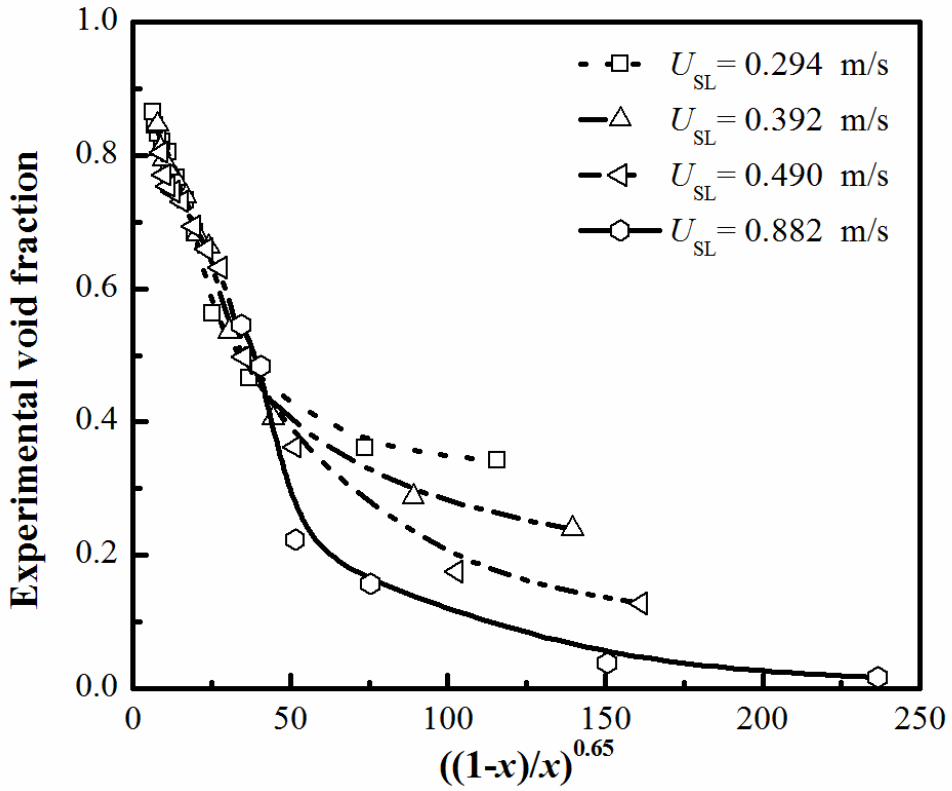

Fig. 16. Variation of the experimental void fraction with the dimensionless parameter $[(1-x)/x]^{0.65}$.

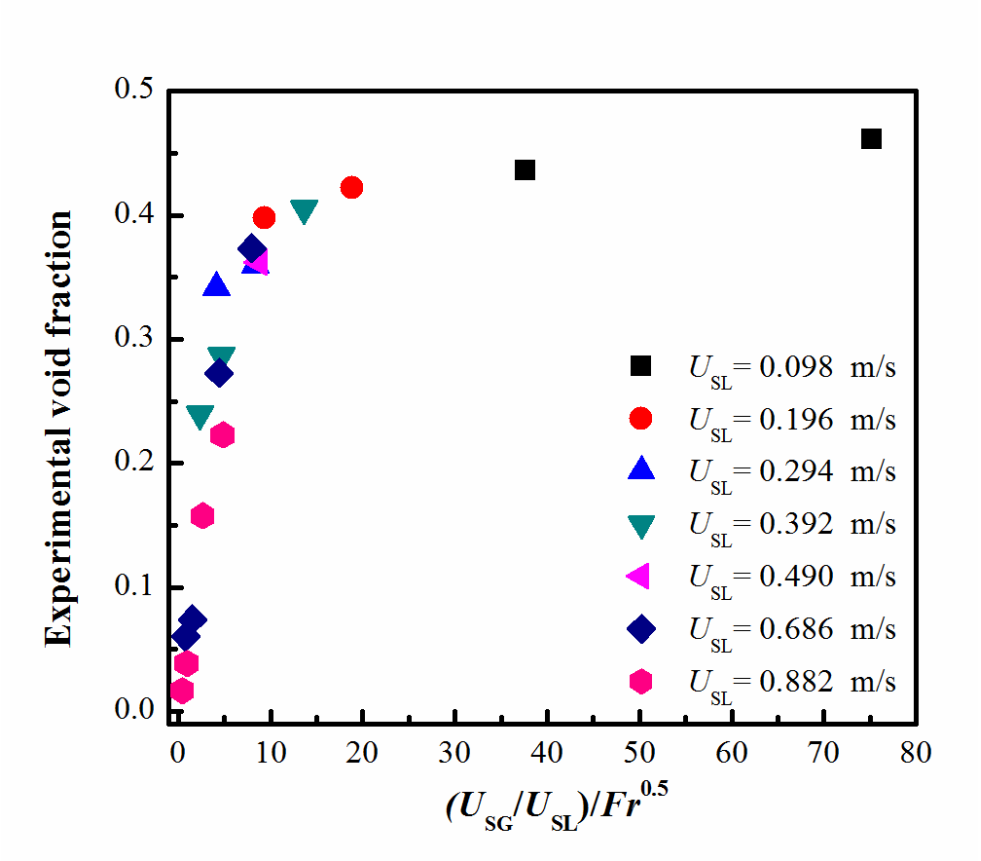

Fig. 17. Variation of the experimental void fraction with the dimensionless parameter of $(U_{SG}/U_{SL})/Fr^{0.5}$.

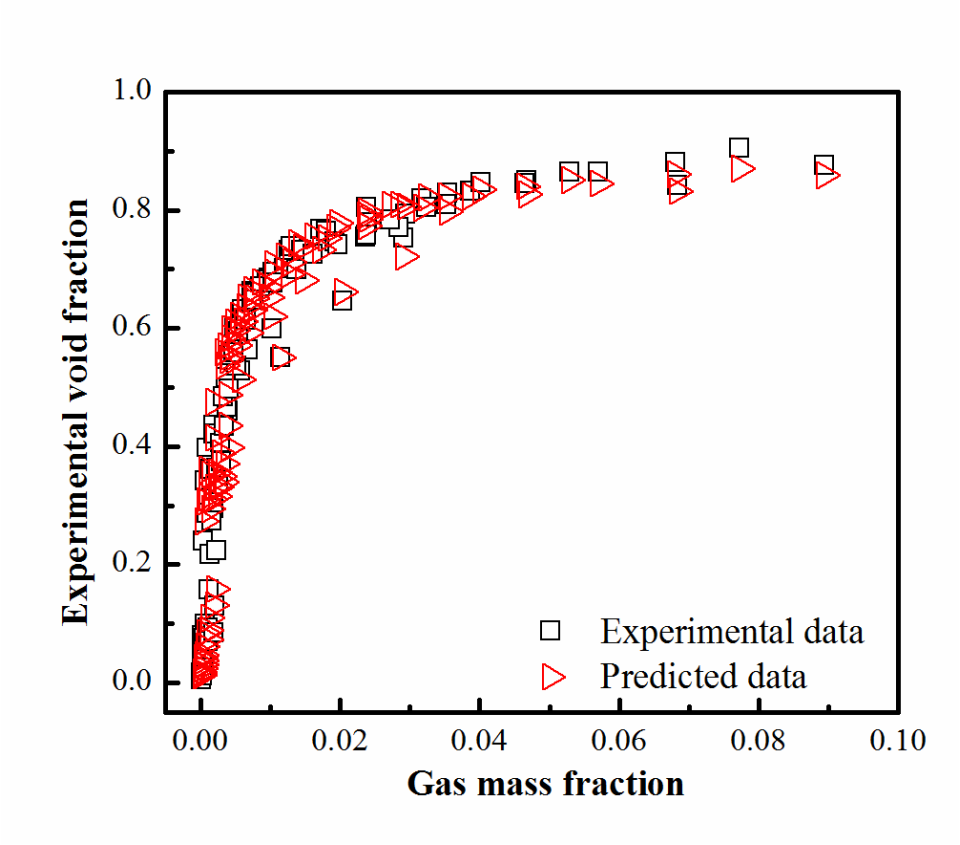

Fig. 18. Variation of the measured average void fraction and the predicted void fraction with the gas mass fraction.

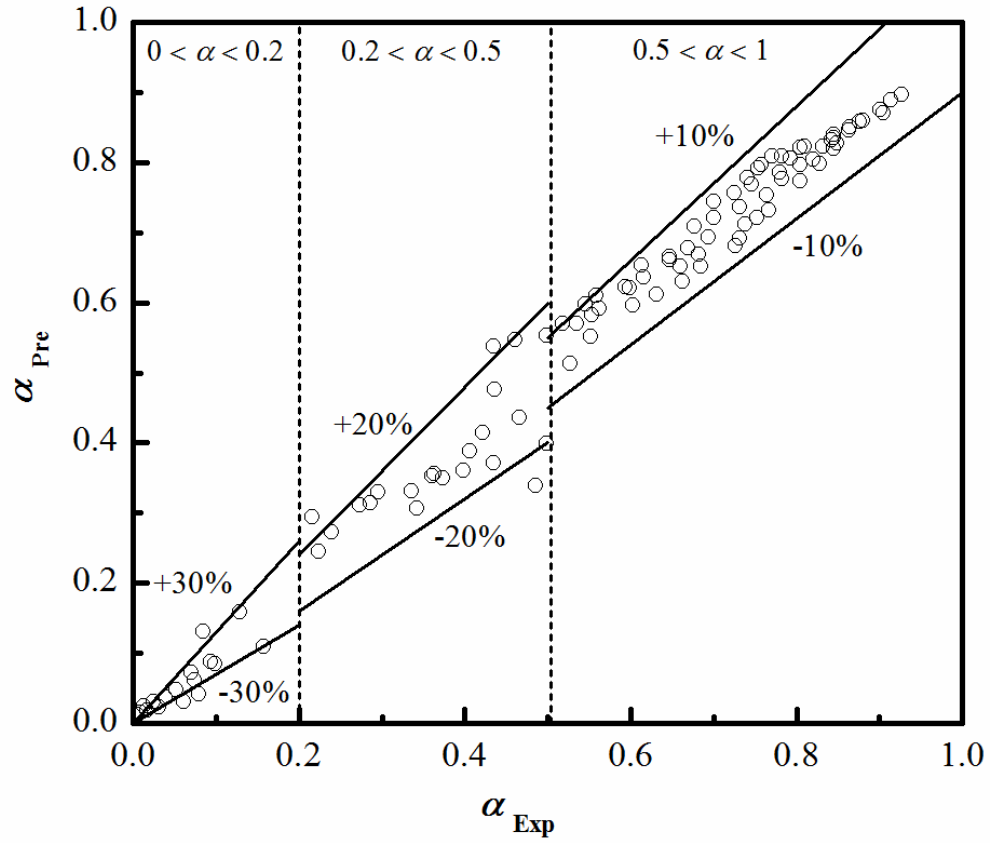

Fig. 19. Comparative results of the measured void fraction to the predicted void fraction with the new proposed models for void fraction the first and second void fraction ranges of $0 < \alpha \leq 0.2$ and $0.2 < \alpha \leq 0.5$ and the recommended model for the void fraction in the range of $0.5 < \alpha \leq 1$.